Journal of Controlled Release 337 (2021) 193–211

Contents lists available at ScienceDirect

Journal of Controlled Release

journal homepage: www.elsevier.com/locate/jconrel

Review article

Advanced mesoporous silica nanocarriers in cancer theranostics and gene editing applications

Kristina Živojević [a], Minja Mladenović [a], Mila Djisalov [a], Mirjana Mundzic [a], Eduardo Ruiz-Hernandez [b], Ivana Gadjanski [a], Nikola Ž. Knežević [a,*]

[a] BioSense Institute, University of Novi Sad, Dr Zorana Djindjica 1, 21000 Novi Sad, Serbia
[b] School of Pharmacy and Pharmaceutical Sciences, Trinity College Dublin, Dublin, Ireland

ARTICLE INFO

Keywords:
Mesoporous silica nanoparticles (MSNs)
Nanotheranostics
Targeted cancer therapy
Cancer imaging
Gene editing

ABSTRACT

Targeted nanomaterials for cancer theranostics have been the subject of an expanding volume of research studies in recent years. Mesoporous silica nanoparticles (MSNs) are particularly attractive for such applications due to possibilities to synthesize nanoparticles (NPs) of different morphologies, pore diameters and pore arrangements, large surface areas and various options for surface functionalization. Functionalization of MSNs with different organic and inorganic molecules, polymers, surface-attachment of other NPs, loading and entrapping cargo molecules with on-desire release capabilities, lead to seemingly endless prospects for designing advanced nanoconstructs exerting multiple functions, such as simultaneous cancer-targeting, imaging and therapy. Describing composition and multifunctional capabilities of these advanced nanoassemblies for targeted therapy (passive, ligand-functionalized MSNs, stimuli-responsive therapy), including one or more modalities for imaging of tumors, is the subject of this review article, along with an overview of developments within a novel and attractive research trend, comprising the use of MSNs for CRISPR/Cas9 systems delivery and gene editing in cancer. Such advanced nanconstructs exhibit high potential for applications in image-guided therapies and the development of personalized cancer treatment.

1. Introduction

Precise and simultaneous personalized chemotherapy is a long-sought research goal in the battle against all types of cancer. This research is driven by different side effects, which are known to occur regularly in all currently applied chemotherapy regimens against cancer. Conventional chemotherapies use highly toxic and reactive molecules as drugs, which may react with the healthy tissues but also exert wide interindividual pharmacokinetic variability with 2–10-fold variations in exposures after standard doses of cytotoxic drugs [1]. Thus, a large portion of introduced drugs may not be capable of reaching the desired cancer tissue, leading to increasing the dosages of chemotherapeutics and subsequently to enhancing their adverse effects. Therefore, a constant balancing between enhancing the activity of drugs and minimizing their undesirable effects, along with inclusion of other drugs for damage mitigation is driving formulations for conventional therapies. Even though novel types of molecular drugs are being developed for targeted cancer therapies, designed to interact selectively with specific features of cancer tissues, these targeted therapies may still be inefficient due to tumor heterogeneity, development of drug resistance and other factors related to unpredictive properties of tumor physiologies in different patients [2].

Developing drug delivery systems (DDS) to overcome limitations and enhance the specificity of anticancer drugs is an ever expanding research area [3–5]. Controlled DDS, aimed at localizing the release and effect of therapeutics, have attracted particular attention [6–8]. A promising strategy to enhance the effectiveness of "precision oncology" lies in combining several cancer-targeting modalities. This may be achieved through application of carefully designed nanocarriers, which may be functionalized with different cancer-specific ligands, aimed to selectively deliver cancer therapeutics, along with simultaneous capabilities for cancer imaging. Different types of nanomaterials are being developed for cancer treatment, with several liposomal, one albumin-based nanovesicle and one hafnium oxide-based nanoparticle approved for clinical use and numerous nanoparticles based on liposomes, proteins, polymers, iron oxide and silica undergoing clinical trials [9,10]. The

* Corresponding author.
E-mail address: nknezevic@biosense.rs (N.Ž. Knežević).

https://doi.org/10.1016/j.jconrel.2021.07.029
Received 17 May 2021; Received in revised form 14 July 2021; Accepted 15 July 2021
Available online 20 July 2021
0168-3659/© 2021 The Authors. Published by Elsevier B.V. This is an open access article under the CC BY license (http://creativecommons.org/licenses/by/4.0/).

differences and advantages between various types of nanocarriers have been detailed in the previous review articles [11–13]. Even though silica-based nanoparticles have not demonstrated superior properties so far in terms of delivery efficiency to solid tumors [14], it is interesting to see how the design of nanoparticles involving silica provides key advantages mainly with respect to stability and drug loading capacity [15–19]. Thus, silica NPs are being increasingly studied as promising cancer-targeting nanocarriers, while the database of clinical studies (https://www.clinicaltrials.gov/) reveals that silica-based nanomaterials, Cornell Dots, are being currently investigated in clinical trials for imaging of nodal metastases, brain and prostate cancer (NCT02106598, NCT03465618, NCT04167969).

Silicon is naturally found in human body, having a beneficial role in bone and connective tissues [20]. Silica nanoparticles, most notably mesoporous silica nanoparticles (MSN), exhibit large surface area and well-structured porosity. The porosity features can be utilized for loading different therapeutics, including nucleotides, targeting molecular drugs, water-insoluble or soluble drugs, imaging agents, as well as their different combinations, which may be simultaneously released within the cancer tissues to enhance their local concentration and achieve synergistic cancer therapy and diagnostics (theranostics) [21,22]. MSNs can be also designed to allow controlled release of loaded cargo in response to an externally applied, cancer tissue-focused stimuli, *e.g.* magnetic field, ultrasound (US) or light, or upon exposure to a weakly acidic extracellular environment of cancer tissues, to the presence of cancer-overexpressed enzymes or other biomolecules [23–27]. Functionalization of the external MSN surface may be utilized for active cancer-targeting, to circumvent the immune system for achieving prolonged presence of the nanocarrier in blood circulation or as moieties for enhancing biocompatibility of nanomaterials. Previous literature reports have described the optimization of MSN features for biomedical applications, highlighting their high biocompatibility, high drug loading capacity, adjustable surface properties and release profiles [28–31].

The possibility to use MSNs as cancer theranostics has also been proposed in the literature [23,32,33]. Herein, we focus our analysis on the studies published since 2015, describing the advanced nanoconstructs with capabilities for concurrent cancer-targeting, treatment and imaging. Selected characteristics of the recent studies on cancer theranostic nanomaterials are summarized in Table 1. In addition, advanced MSN-based strategies for cancer therapy through gene editing are reviewed, considering the significance of the topic, spotlighted by the 2020 Nobel prize in Chemistry "for the development of a method for genome editing" awarded to Emmanuelle Charpentier and Jennifer A. Doudna.

2. Targeted therapy of cancer

Targeting cancer through the application of nanomedicines can be achieved by passive and active mechanisms [78–81]. Passive targeting can be rationalized as the accumulation of NPs within cancer tissues by means of the enhanced permeability and retention (EPR) effect [82]. Active targeting includes all targeting that is achieved beyond the EPR effect, which may involve modifications of the surface of nanoparticles with ligands for specific interaction with overexpressed receptors, through designing nanosystems for triggering the drug release by exploiting overexpressed biomolecules or the weakly acidic extracellular environment in tumors [83], or through externally applied stimuli, such as light irradiation, magnetic field or US [84–87].

2.1. Passive cancer targeting with MSNs

The EPR was discovered by Matsumura and Maeda over three decades ago [29,88]. The EPR effect occurs due to the rapid growth of the tumor, which further leads to the creation of new blood vessels (*i.e.* neoangiogenesis) necessary to supply the tumor tissue with a sufficient amount of oxygen and nutrients needed for its further proliferation. In general, cancer cell death will initiate the secretion of growth factors that promote the formation of new blood vessels from the surrounding capillaries. This will further lead to the extremely rapid development of new, irregular blood vessels showing a discontinuous and single thin layer of flattened endothelial cells with the absence of a basement membrane. Thus, NPs can leave blood vessels and penetrate the adjacent tumor tissue through the discontinuous leaking membrane (Fig. 1). This effect does not apply to normal, healthy tissue in which the fluid in the bloodstream is constantly subjected to lymphatic drainage. The efficiency of the drainage system is suppressed significantly in tumors, directing to enhanced retention of NPs in tumor tissues [29,78,79].

The effectiveness of passive cancer-targeting may differ for NPs having different sizes, shapes, and surface properties. The size of MSNs plays an essential role in blood circulation, biodistribution, penetration into tissues, and cell internalization. Namely, the two main pathways of elimination of injected MSNs include the reticuloendothelial system (RES) and renal clearance [79]. According to Waterman and Brieger, MSNs must be at least 10 nm in diameter to avoid renal clearance, while the size of 100–200 nm is considered optimal for avoiding RES and achieving efficient accumulation and retention in the tumor matrix mediated by the EPR effect [90].

A number of studies demonstrate that the shape of NPs plays a significant role when it comes to cellular interaction and systemic biodistribution [91–93]. Li and coworkers investigated MSNs with an aspect ratio of 1, 1.75 and 5 on their *in vivo* biodistribution, excretion and toxicity after oral administration [92]. The results showed that *in vivo* biodegradation decreased, absorption of MSNs by the small intestine and other organs decreased and the urinary excretion increased, with the increasing aspect ratio. Shao et al. studied the effects of MSNs with aspect ratios 1, 2, and 4 upon intravenous injection into tumor bearing mice, to determine their destination *in vivo* [93]. The MSNs were mostly detected in the RES organs including liver, spleen and kidney, with spherical MSNs preferentially detected in the liver, while long-rod MSNs exhibited more retention in the spleen. In general, rod-like MSNs exhibited enhanced accumulation within tumor tissue in comparison to the spherical MSNs.

The surface properties of MSNs have an impact as well on achieving effective passive targeting. Namely, overly hydrophobic or charged systems can be rapidly opsonized by the mononuclear phagocyte system (MPS). Manipulation of the surface properties of MSNs can dictate the time (prolongation) of the circulation of these NPs in the bloodstream, as well as a decrease in renal clearance [94]. Nude (*i.e.* unfunctionalized) MSNs are characterized by exposed silanol groups on their surfaces, which are negatively charged under physiological conditions. These surface silanol groups will tend to interact with the erythrocyte membrane, which could lead to hemolysis [79]. However, due to their lower density of surface silanol groups, some studies suggest that MSNs have lower hemolytic activity than amorphous silica [95], which can be further reduced by incorporating organic components into the silica framework [96,97].

In 2010, He et al. showed that PEGylation of MSNs reduces nonspecific binding of serum proteins and cellular responses [98]. Today, PEGylation is considered the most effective strategy for modifying NPs to significantly increase the half-life by delaying opsonization. Besides, PEGylation has been found to reduce the distribution of MSNs in the liver and spleen, as well as to prolong the life of MSNs in blood circulation and reduce the rate of excretion [99].

Sweeney et al. injected mice with PEG-functionalized MSNs, also containing Gd_2O_3 for magnetic resonance imaging (MRI) [100]. Three hours after injection of functionalized MSNs, there was a difference of the T2-weighted signal in kidneys of the treated group, appearing dark relative to the surrounding tissue, in the area where formed urine collects. However, no accumulation of particles was detected in the renal cortex where glomerular filtration takes place. Free floating MSNs (mean hydrodynamic diameter of 187 nm) were cleared by the kidneys within 3 days based on the timing of MRI intensity changes.

Table 1
Overview of recent studies on MSN-based cancer theranostic nanomaterials.

Composition	Drug delivered	Cancer type	Method of therapy	Method of imaging	Method of targeting	Ref.
Poly (tannic acid) modified MSN	DOX	Breast cancer	pH	NIRF	HER2 antibody, pH-responsive	[34]
Lipid-coated MSN	Irinotecan	Hepatocellular carcinoma	pH	NIRF	Galactosyl, pH-responsive	[35]
MMSN	DOX	Breast cancer, cervical carcinoma	Redox	T2-weighted MRI	Arg-Gly-Asp (RGD), redox-responsive	[36]
Core/shell $Cu_{1.8}S$/MSN	DOX and curcumin	Breast cancer	NIR	Infrared thermal imaging	Aptamer GC-rich DNA helix, NIR responsive	[37]
Two-photon sensitive PMO	DOX	Breast cancer	NIR	TPF	NIR-responsive	[38]
HMON phagocytosed into macrophage	DOX	Breast cancer	HIFU-induced hyperthermia	US enhanced echo signal	Macrophage natural migration toward cancerous cells	[39]
Core/shell MSN, UCNPs	DOX and camptothecin	Cervical and breast cancer	ATP-responsive	LRET	FA	[40]
Dual-porous mesoporous silica-coated mesoporous carbon NPs	DOX	Breast cancer	pH/redox/NIR	Photothermal	pH/redox/NIR multi-responsive	[41]
MMSN	DOX	Breast cancer	pH/redox	T2-weighted MRI	citraconic anhydride, pH, redox	[42]
MMSN	DOX	Fibrosarcoma	MMP-2 enzyme responsive peptide	T2-weighted MRI	MMP-2 substrate peptide, enzyme	[43]
MSN-coated $Mn_{0.6}Zn_{0.4}Fe_2O_4$	DOX	Breast cancer	Magnetothermal, chemodynamic	T2-weighted MRI	Magnetic field	[44]
MSN with Gd_2O_3	DOX	Liver cancer	pH	T1-weighted MRI	FA, pH	[45]
Zn^{2+}-Doped Fe_3O_4 Core/MSN	DOX	Cervical cancer	pH	T2-weighted MRI	FA, pH	[46]
MSN labeled with ^{68}Cu radioisotope	CpG and photosensitizer chlorine e6 (Ce6)	Colon carcinoma	Redox	PET	neoantigen peptides (ADP-dependent glucokinase, Adpgk), redox	[47]
Au@Gd_2O_3@MSN		Breast cancer	Photothermal	MRI and TPF	FA, light responsive	[48]
MSN	Tirapazamine	Squamous cell carcinoma	Enzyme	NIR fluorescence and MRI	Hyaluronic acid, enzyme responsive	[49]
Alginate/chitosan MMSN with Au and iron oxide bifunctional core	DOX, Ce6	Breast cancer	pH, PDT	CT/MRI	magnetic targeting, pH	[50]
Au nanostar -coated HMSN		Glioma	PTT	US/CT/PA/ Thermal	light responsive	[51]
Gd doped-MSN	DOX	Breast cancer	PTT	NIRF, PA and MRI	FA, light responsive	[52]
PFH-encapsulated PDA-MSN	ICG, PFH	Breast cancer	PTT/PDT	US and NIRF	FA, light responsive	[53]
^{99m}Tc- MnOx-MSN	DOX	Breast cancer	pH	SPECT/MRI	pH responsive	[54].
QD yolk/shell HMSN	DOX	Breast cancer	pH	PET/optical	chimeric antibody TRC105, pH responsive	[55]
PMO coated Prussian blue	DOX	Breast cancer	pH and photo heating	MRI and PA	pH and light	[56]
MSN-coated Au nanorods	5-fluorouracil	Melanoma	pH, NIR, PDT, PTT	TPF, PA, PTI	pH and light	[57]
Wormhole MSN	Carboplatin or paclitaxel	Ovarian cancer	pH	MSOT	low pH insertion peptide V7, pH-responsive	[58]
Rattle-structured PDA-MSN	Chloroquine	Hepatocellular carcinoma	NIR irradiation PTT	PA	NIR responsive	[59]
Superhydrophobic MSN	DOX	Transgenic adenocarcinoma of mouse prostate	Chemotherapy, sonodynamic therapy	US	US-responsive	[60]
^{99m}Tc radio-labeled MSN	DOX	Triple-negative breast cancer	Enzyme	SPECT	MUC1 aptamer, enzyme	[61]
PEGylated MSN–titania NPs		Squamous cell carcinoma	US-responsive ROS generation	PA	US	[62]
$MnFe_2O_4$-decorated large pore MSN- lanthanide UCNPs		Hepatocellular carcinoma	PDT	UCL imaging/MRI	Light	[63]
Zn and Mn-doped MSN		Glioma	X-ray-induced PDT	X-ray imaging	RGD peptide, X-ray	[64]
MSN-UCNPs	DOX	Hepatocarcinoma	pH, PDT	Upconversion/MRI	FA, pH, light	[65]
$MnFe_2O_4$-MSN		Glioblastoma	PDT in hypoxic cancer	MRI	Light	[66]
MSN-Au		Breast cancer	Acidity induced NIR PDT/PTT	PTI	RLA peptide (Ada-GG-$(RLARLAR)_2$), light	[67]
MSN-Au	Cisplatin/Avastin	Cervical cancer	NIR irradiation PTT	PTI/MRI	AE105 peptide, light	[68]
ICG and catalase loaded dendritic MONs	ICG	Breast cancer	PDT	PA/US	Light	[69]
PMO coated with Prussian blue NPs	5-ALA	Glioma	PDT	T2-weighted MRI, fluorescence	Light	[70]
MMSN loaded with UCNPs		Breast cancer	NIR PDT/PTT	NIR PA/UCL	Magnetic targeting, light and FA	[71]
MSN@Au, Gd-TPPS	Gd-TPPS	Breast cancer	PDT/PTT	NIRF/MSOT/CT/ MRI	Light	[72]
CuS-^{89}Zr HMSN loaded with porphyrin	TCPP, CuS, DOX	Breast cancer	PTT/PDT	PET/FL/CL/CRET	Light	[73]
HMONs, Mn-protoporphyrin (PpIX)	Mn-PpIX	Breast cancer	Sonodynamic	T1-weighted MRI	US-responsive	[74]

(*continued on next page*)

Table 1 (*continued*)

Composition	Drug delivered	Cancer type	Method of therapy	Method of imaging	Method of targeting	Ref.
EuGdOx-doped MSN frameworks	DOX, EuGdOx	Melanoma	NIR light triggered chemo and PDT	Fluorescence/MRI	FA, NIR-responsive	[75]
BSA-Gd capped MSN-ss-HA	DOX	Breast cancer	Redox	MRI	HA-targeting, Redox-sensitive	[76]
PEGylated core/shell CuS@MSN	DOX	Breast cancer	pH-responsive	PET	TRC105-based vasculature targeting, pH-responsive	[77]

5-ALA – 5-aminolevulinic acid, ADP – Adenosine diphosphate, ATP – Adenosine triphosphate, BSA – Bovine serum albumin, Ce6 – Chlorine e6 photosensitizer, CT – Computed tomography, DOX – Doxorubicin, FA – Folic acid, HA – Hyaluronic acid, HIFU – High-intensity focused ultrasound, HMONs - Hollow mesoporous organosilica nanoparticles, HMSN – Hollow mesoporous silica nanoparticles, ICG – Indocyanine green, LRET – Luminescence resonance energy transfer, MMSN – Core/shell magnetic mesoporous silica nanoparticles, MONs – Mesoporous organosilica nanoparticles, MSN – Mesoporous silica nanoparticles, MRI – Magnetic resonance imaging, MSOT – Multispectral optoacoustic tomography, NPs – Nanoparticles, NIR – Near-infrared, NIRF – Near-infrared fluorescence imaging, PA – Photoacoustic imaging, PDA – Polydopamine, PEG – Polyethylene glycol, PFH – Perfluorohexane, PDT – Photodynamic therapy, PET – Positron emission tomography, PMO – Periodic mesoporous organosilica, PTI – Photothermal imaging, PTT – Photothermal therapy, QD – Quantum dot, ROS – Reactive oxygen species, SPECT – Single-photon emission computed tomography, TCPP – (4-carboxyphenyl)porphyrin, TPPS – Tetraphenylporphine sulfonate, TPF-Two-photon fluorescence, UCL – Upconversion luminescence, UCNPs – Upconversion nanoparticles, US – Ultrasound.

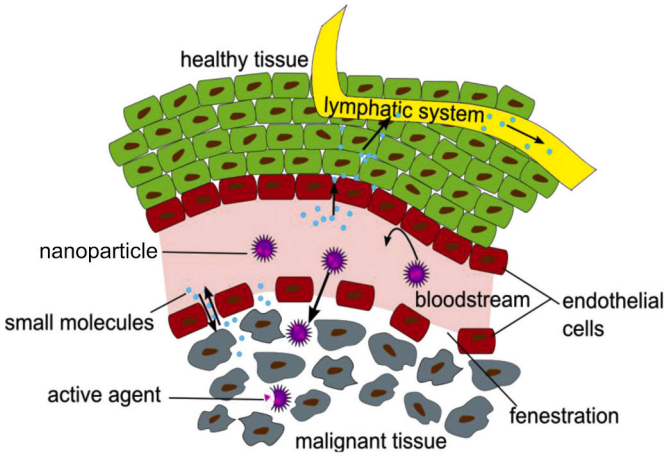

Fig. 1. Schematic representation of the selective accumulation of NPs in malignant tissues through the EPR effect and delivery of active agents. Adapted with permission [89].

In vivo biocompatibility of MSNs and their capabilities for tumor-targeted treatment were first demonstrated in 2010 by Lu et al. [101] Since this initial investigation, different authors reported detailed *in vivo* studies, which need to be conducted on each novel nanoconstruct, as any change in structure and surface properties of MSNs influence their *in vivo* behavior. For example, biocompatibility and biodistribution of redox/pH/NIR multi-responsive doxorubicin (DOX) delivery system based on MSN grafted with polydopamine (PDA) *via* disulfide bonds (MSN-SS-PDA/DOX) was tested in experiments on 4 T1 tumor-bearing mice [102]. Free DOX and MSN-SS-PDA/DOX suspensions containing 10 mg kg^{-1} DOX were injected through the tail vein and biodistribution results showed that in the case of the free DOX group, the concentration of DOX in the tumor reached a maximum at 2 h post-injection, and then gradually decreased. On the contrary, upon the treatment with MSN-SS-PDA/DOX, the concentration of DOX showed a maximum value at 6 h post-injection, which could be attributed to the EPR effect. In addition, the treatment with free DOX evidenced therapeutic effects but also toxicity to healthy tissues, while the treatment with constructed nanomaterial showed high biocompatibility against healthy tissues and potent anticancer activity upon the stimuli-induced DOX release.

2.2. Active targeting of overexpressed receptors in cancer tissues

Once the size and shape of MSNs are optimized, their capability for targeting tumor tissues can be further enhanced by modifying their surface with cancer-specific ligands [29]. Ligand-modified MSNs can recognize receptors that are selectively expressed or overexpressed on tumor cell membranes, leading to the enhancement of antitumor selectivity [90,103]. Different types of molecules are used for these purposes: peptides, aptamers, antibodies, proteins, polysaccharides, small molecules, and others (Fig. 2).

Peptides containing the RGD motif (Arg-Gly-Asp) are widely used for targeting cancer, which is due to their strong and selective interaction with αvβ3 integrins [104,105]. Integrins belong to heterodimeric cell surface receptors that mediate adhesion to extracellular matrix (ECM) and immunoglobulin superfamily molecules. Their role in the regulation of a diverse array of cellular functions, crucial to the initiation, progression and metastasis of solid tumors is well known. The most investigated integrins in cancer research are αvβ3, αvβ5, a5β1, a6β4, a4β1 and αvβ6 whose overexpression is in correlation with disease progression in various tumor types [106]. Another frequently used targeting motif is NGR (Asn-Gly-Arg) peptide, which targets tumor neovasculature by specifically binding to the metalloprotease aminopeptidase N receptor (also known as CD13, APN receptor) [107]. CD13 is commonly overexpressed in tumor cells and is associated with neoangiogenesis and cancer progression. It is identified as a cell-surface marker for malignant myeloid cells and investigations showed that it reached high levels of expression correlated with progression in various cancer types, including breast, ovarian, and prostate [108].

One more group of peptides which can be used for effective tumor-targeting are **cell-penetrating peptides** (CPPs) [109]. CPPs are small

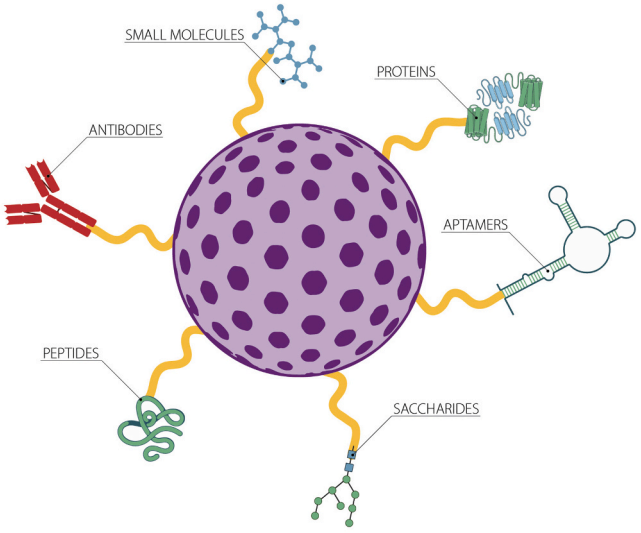

Fig. 2. Schematic representation of different types of functional groups that could be functionalized on MSNs for active cancer-targeting.

(5–30 amino acids) peptides that are increasingly used to decorate NPs to design constructs for active tumor-targeting. Decoration of NPs with CPPs can improve NPs potential under physiological conditions and enhance their cellular uptake. CPPs, which are often cationic, allow translocation across biological membranes to allow targeted delivery to intracellular target sites through NP-CPP conjugates [110]. A **low pH insertion peptide** (pHLIP) called V7 is also applicable for targeting cancer. Endocytosis of pHLIP-functionalized NPs is not favored unless Asp residues of this peptide get protonated at weakly acidic pH of tumor microenvironment [107,108].

Proteins involved in the accelerated metabolism of cancer cells, such as transferrin (Tf), which participates in the transport of iron into cells, and Epidermal Growth Factor (EGF), which stimulates cell growth and differentiation, can be also used to target tumor cells [111]. Iron is known as a key element associated with various physiological and pathological processes. The disturbance of its metabolic balance can be associated with various serious diseases, including cancer. Transferrin is a plasma iron-binding protein which binds to transferrin receptors (TFRs), TFR1 and TFR2. TFR1 is ubiquitously expressed, and its levels are regulated by cellular iron levels, whereas TFR2 is mainly expressed in the liver and its levels are regulated by transferrin saturation. TFR1 is referred to in the literature as a receptor that is overexpressed in various cancers [112]. On the other hand, understanding the physiological function of Epidermal Growth Factor Receptors (EGFR) is extremely important because it explains why EGF is increasingly being used to modify NPs for the active targeting of cancer cells. The main role of EGFR is regulating the development of epithelial tissue and homeostasis that are disrupted in pathological conditions. Different types of cancers arise from mutation and overexpression of EGFR, which is why EGFR are increasingly used as targets in multiple cancer therapies currently adopted in clinical practice [113]. Vascular endothelial growth factor (VEGF) is also one of the most attractive target proteins, often used for cancer targeted therapy. This is mainly a consequence of its easy access since it circulates in the blood and acts directly on endothelial cells. Besides, VEGF is a key mediator of neoangiogenesis, the process of forming new blood vessels necessary to provide nutrients and oxygen to tumor cells [114].

Antibodies are regarded as highly specific and efficient targeting ligands, where the monoclonal antibodies (or their fragments) are often used for cancer therapy. Among the antibodies circulating in the serum (IgG, IgA, IgM, IgE), IgG is the main antibody used for cancer therapy and diagnosis. It has a Y-shaped structure of which the two arms of the structure contain antigen recognition sites, and the stem structure brings about effector functions [115]. Even though their interaction with antigens may be influenced upon attachment to nanomaterials and their presence may instigate early clearance of the functionalized NPs [116], there is an increasing number of studies describing the use of antibodies as cancer-targeting components. For example, Dréau et al. reported the development of NIR emitting dye-doped MSNs, conjugated to a tumor-specific MUC1 antibody (ab-tMUC1-NIR-MSN) for *in vivo* optical detection of breast adenocarcinoma tissue [117]. Additionally, Goel et al. conducted a study in which the targeting of CD105-specific vascular tumors was successfully demonstrated in a mouse model of metastatic breast cancer using biodegradable MSNs conjugated to TRC105 (antibody to CD105) [118]. A complex MSN-based nanoconstruct, containing PEGylated core/shell CuS@MSN for photothermal therapy (PTT), chelated ^{64}Cu for PET imaging and TRC105 antibody for targeting tumor neovasculature (^{64}Cu-CuS@MSN-TRC105), was demonstrated *in vivo* for long-term biocompatibility at a high dosage of 90 mg kg^{-1} on tumor-bearing mice [77]. After intravenous injection, two months after the treatment, tissues from the heart, liver, spleen, lung and kidney were investigated for potential signs of toxicity, but no histological differences were observed between the treatment and control groups.

For cancer-targeting purposes, an antibody for the enzyme carbonic anhydrase (CA) IX is also applicable, as it is expressed on the surface of cancer cells with limited expression in healthy tissues [119]. These enzymes are considered as very important in mediating the pH of tumor cells, by modulating the concentration of bicarbonate and protons for cell survival and proliferation. Namely, there are 12 active CA isoforms, two of which, CA IX and XII, are considered as effective anti-cancer targets [120].

Aptamers are short (12–80 nt) single-stranded oligonucleotides generated by SELEX (Systematic Evolution of Ligands by Exponential Enrichment) technology, that can bind to a specific target molecule with high specificity and affinity. Aptamers are frequently termed as "chemical antibodies" since their function is similar to conventional antibodies. However, aptamers are quite smaller, can be synthesized in a much faster and less expensive way, can be chemically modified in various ways, have flexible structure and low immunogenicity [121]. Furthermore, many aptamers are internalized upon binding to the ligands on the cell surface, which makes them a suitable tool for targeted delivery to the specific cells [122].

Li et al. developed anti-miR-155-loaded MSNs modified with polydopamine (PDA) and **AS1411 aptamer** for the targeted treatment of colorectal cancer (CRC) [123]. MicroRNA-155 (miR-155) is an oncogenic miRNA, overexpressed in many cancers, including CRC. Hence, the authors aimed to deliver the anti-miR-155 (a specific microRNA that suppresses expression of miR-155) *via* the MSNs functionalized on the surface with the SH-terminated AS1411 aptamer. The AS1411 is a 26 nt G-rich DNA aptamer and the first aptamer approved by the US Food and Drug Administration [124]. AS1411 is used to target the tumor cells since it specifically binds to nucleolin, which is overexpressed on the cell surface in CRC as well as in many other tumors. An additional benefit is achieved *via* PDA coating, enabling pH-sensitive controlled release of the MSN-cargo in the acidic environment of the tumor. Targeted delivery of the MSNs-anti-miR-155@PDA-AS1411 efficiently down-regulated miR-155 expression in SW480 cells (human CRC cell line) and achieved high targeting efficiency and enhanced therapeutic effects in both *in vivo* and *in vitro* experiments.

Tang et al. have developed a system for photo-reactive delivery of DOX, based on the non-covalent assembly of cancer-targeting **Ci5.5-AS1411 aptamer** on graphene oxide (GO), which is also used as the light-responsive pore-blocking moiety, for the entrapment and delivery of DOX (MSN-DOX@GO-Apt) [125]. Hanafi-Bojd et al. developed a **MUC-1 aptamer**- conjugated MSNs for targeted delivery of epirubicin to breast cancer cells [126]. The MUC1 aptamer selectively binds to abnormally glycosylated mucin-1, which is expressed on various cancer cells including breast, ovarian, pancreas, prostate, colon and lungs.

Another aptamer that is often used to decorate the surface of NPs for the active targeting of cancer is the aptamer for human epidermal growth factor receptor-2 (HER2) - also known as HApt aptamer [112]. Amplification or overexpression of HER2 occurs in approximately 15–30% of breast cancers and 10–30% of gastric/gastroesophageal cancers and serves as a prognostic and predictive biomarker [127]. Overexpression of HER2 has also been found in other cancer types like ovary, endometrium, bladder, lung, colon, and head and neck. An example of the use of HApt aptamer for decoration of MSNs was proposed by Zhang et al., who demonstrated the capabilities of HApt aptamer to act as a targeting agent and as an antagonist to maximize the efficacy of MSN-based DDS for HER2-positive breast cancer [128].

Polysaccharides are also a class of molecules that are increasingly used as biodegradable, hydrophilic agents to decorate MSNs for active cancer-targeting. The most commonly used polysaccharides for this purpose include chitosan, dextran, and hyaluronic acid (HA) - most often mentioned in the literature due to their specific interaction with CD44 and CD168 receptors involved in many types of cancer [129–131]. For example, due to the specific binding of HA to CD44, DOX-HA-MSN nanocarriers showed enhanced cytotoxic activity against 4 T1 breast cancer cells compared to normal GES-1 gastric mucosal cells [132]. Zhang & Xu have developed multifunctional envelope-type nanodevices (MEND), which can specifically target cancer cells and respond to

upregulated extracellular matrix metalloproteinase-2 (MMP-2) in tumors while providing an enhanced cellular internalization *via* HA receptor-mediated endocytosis [133].

The use of **small molecules**, *i.e.* molecules of a low molecular weight (typically <1000 Da), for cancer-targeting is also attracting attention due to their simple structure and low cost. This primarily refers to vitamins - natural or from synthetic sources. The most used targeting element is folic acid (FA, vitamin B9) [134], which can be attached to MSNs through a facile amidation of amino-organosilanes [135]. This type of active targeting is made possible by the specific binding of FA to folate receptors, overexpressed in many tumors compared to healthy tissues [29]. Khosravian el al. reported the capability of docetaxel (DTX)-loaded folic acid-functionalized MSNs to target breast cancer tissues *in vivo* [136]. In addition to FA, many studies describe the use of other vitamins such as biotin (vitamin B7 or H) or cyanocobalamin (vitamin B12) for decoration of MSNs, to construct cancer-targeting DDS [137–139]. Additionally, synthetic small molecules such as phenylboronic acid (PBA) are implemented for targeting cancer by MSNs as well [140]. Mannose and Mannose-6-phosphate are also being applied in cancer targeting [141], Due to the high demand of nutrients needed for their rapid proliferation, cancer cells have very high affinity for carbohydrate molecules compared to normal cells, and mannose receptors are overexpressed by tumor-associated macrophages [142]. These conditions enable the use of different Si-based nanoparticles for application in cancer-targeted theranostics [143–145].

2.3. MSN based nanomaterials for pH-responsive targeted cancer theranostics

Oncogenic metabolism generates a large amount of lactate, excess protons, and carbon dioxide, altogether leading to increased acidification of the extracellular tumor microenvironment [146]. Consequently, the extracellular environment of cancer cells has lower pH compared to normal cells [147]. It is considered that low extracellular pH helps tumor progression, metastasis, resistance to therapy and inhibition of immunological response [148]. The average intracellular pH (pH_i) of both tumor and normal tissue is 7.2, while the extracellular pH (pH_e) is 7.4 in the normal tissue and in tumors is typically measured in the range 6.8–7.2, and even lower [147]. Researchers have been reporting on various strategies for designing the most efficient pH-sensitive MSN-based drug carrier. One of the principal, widely examined methods, is the introduction of a pH-responsive linker for binding a pore capping agent [149–151]. For example, acid-responsiveness of an acetal linker was utilized for loading and release of DOX from MSNs, capped with polyacrylic acid [152]. Another possibility is to use a hydrazone bond, as in the case of the photosensitizer zinc(II) phthalocyanine (ZnPc) bound to stellate mesoporous silica (SMSN) to achieve controlled and enhanced PDT of cancer [153]. The conjugation of ZnPc onto SMSN resulted in quenching the fluorescence emission and inhibiting reactive oxygen species (ROS) generation, whereas photodynamic properties were established again once the photosensitizer was released.

pH-responsive shells for MSNs have been explored as well, such as reversible pH-sensitive shell for drug delivery [34]. MSNs loaded with DOX and with a polymer shell composed of tannic acid/tetraethylenepentamine (TA/TEPA) were shown to swell reversibly upon changing the pH, which enabled enhanced release of DOX at pH 6.8 and pH 5, *versus* the release at physiological pH. The nanomaterials were also functionalized with HER-2 antibody as a targeting ligand, which was demonstrated by *in vivo* studies to facilitate the accumulation of NPs in cancer tissues and to effectively inhibit tumor growth through targeted DOX delivery. Likewise, the lipid-based coating was demonstrated as a pH-responsive shell for MSNs [35]. The lipid shell was composed of (2E)-4-(dioleostearin)-amino-4-carbonyl-2-butenonic (DC), which changes its charge in weakly acidic environment from negative to neutral. The lipid shell also incorporated galactosyl-conjugated PEO-PPO-PEO surfactant (P123) for targeting hepatocellular carcinoma (HCC). Enhanced release of antitumor drug irinotecan (CPT-11) was demonstrated from MSNs in weakly acidic conditions, in addition to enhanced tumor uptake and selective drug delivery to tumor by *in vitro* and *in vivo* studies.

Imaging modality incorporated into a nanoplatform provides novel materials with advanced properties for treatment guidance, monitoring of pharmacokinetics, simplified and personalized cancer treatment with potentially more successful outcomes. The development of novel theranostic nanovectors that can be used for on-demand delivery of therapeutic agents combined with simultaneous non-invasive imaging techniques is the focus of interest in the paper by He et al. [154] MSNs were co-loaded with gadolinium oxide (Gd_2O_3), a well-known MRI contrast agent, and DOX to give Gd_2O_3@MSN-DOX. In order to prevent cargo leakage, the composite was capped with pH-responsive polyelectrolytes. Once the as-synthesized composite reaches the cancer cell with acidic pH, the surface copolymer undergoes a pH-triggered charge reversal process, which disintegrates the polyelectrolyte layer and induces cargo release. The nanoplatform was modified with FA to ensure cancer-targeting and enhanced cancer uptake. *In vivo* testing on VX-2 tumor-bearing rabbits showed a persistent elevation in T1-weighted signal intensities within 1 week after intratumoral injection and 50.2% of apoptotic cells 48 h after the treatment.

Dual-modal upconversion/MR imaging was demonstrated by core/shell structured mesoporous silica-coated gadolinium-doped upconversion NPs [65]. Photosensitizer Rose Bengal (RB) was incorporated within the silica shell and the external surface was decorated with a zeolitic imidazolate framework-90 (ZIF-90). Finally, DOX and amino-PEG modified FA were covalently attached to ZIF-90, to enable targeted chemotherapy. At weakly acid conditions ZIF-90 is degraded, which releases oxygen for achieving synergistic chemotherapy and oxygen-enhanced PDT. Further, upconversion NPs exhibited a luminescence signal upon excitation at 808 nm, suitable for fluorescence microscopy, while MRI contrast enhancement was enabled due to Gd-doping, which makes the described nanomaterial an excellent candidate for dual-modal imaging.

Novel theranostic nanoplatform based on wormhole MSNs as a dual targeting system for the lower extracellular pH was recently developed [58]. Silica NPs with asymmetric wormhole pores were synthesized, the pores were loaded with paclitaxel or carboplatin and capped by a pH responsive gatekeeper chitosan (pK_a of 6.5), which gets protonated at the weakly acidic environment and enables the cargo release. The resulting composite was further conjugated with a low pH insertion V7 peptide for cancer targeting purposes. Multispectral optoacoustic tomography (MSOT) modality was also enabled through loading the pores with IR780 imaging dye, for efficient targeted theranostics of ovarian cancer *in vitro* and *in vivo*.

Core/shell magnetic MSNs, containing Au and iron oxide bifunctional core, photosensitizer chlorine e6 (Ce6) and DOX loaded inside the pores was also reported [155]. Alternating polyelectrolyte multilayers of alginate and chitosan acted as pH-sensitive gatekeepers, while the P-glycoprotein short hairpin RNA (P-gp shRNA) was attached electrostatically, for battling multidrug resistance. Dual-modal imaging – MR and computed tomography (CT) imaging, is enabled by Fe_3O_4-Au combination in the core of these NPs while *in vivo* synergistic anti-tumor effects were achieved by chemo-photodynamic combined gene therapy. FA-functionalized magnetic core/shell MSNs for simultaneous MRI and tumor-targeted, pH-responsive DOX delivery was developed containing superparamagnetic iron oxide nanoparticle (SPION) core doped with Zn^{2+}, which improved saturated mass magnetization values providing significant contrast ability in T2-weighted MRI [46].

The development of dual nanoprobes combining single-photon emission computed tomography (SPECT) and MRI was also of interest for cancer imaging [156], as SPECT is characterized by outstanding sensitivity, whereas MRI shows high spatial resolution. For this purpose, ^{99m}Tc was labeled on the surface of manganese oxide-based MSNs and *in vivo* MRI measurements showed significant T1-contrast enhancement

15 min p. i., reaching its maximum signal intensity at 3 h post injection. T1-weighted MRI performance was caused by the gradual accumulation of nanocomposites in the tumor tissues and the release of Mn^{2+} triggered by the weakly acidic tumor microenvironment, which was also followed by the enhanced DOX delivery. A quantum dot (QD) yolk/shell-structured hollow mesoporous silica nanosystem, functionalized with a chelated ^{64}Cu radioisotope and cancer-targeting TRC105 antibody, was also employed for tumor vasculature targeting, dual-modal positron emission tomography (PET)/optical imaging and pH-sensitive drug delivery [55].

2.4. MSN-based redox-responsive targeted theranostics of cancer

Glutathione (GSH) is an intracellular reducing agent, which plays a significant role in the control of the redox state of cells and its concentration is an important factor in determining the redox environment [157]. Cancerous cells suffer from oxidative stress due to increased ROS generation, which often leads to redox compensation and upregulation of GSH, among different other antioxidant molecules [158]. As studies showed that intracellular GSH level in tumor cells is higher than in healthy cells [159], this feature can be exploited for selective drug delivery to cancer tissue. Disulfide linker is the most widely used redox-sensitive linker [160]. For instance, Chen's group reported MSN-based nanocarrier for redox-responsive DOX delivery by exploiting disulfide linkage established between MSNs and a targeting ligand, anti-carbonic anhydrase IX antibody (A-CAIX Ab) [161], which also serves to block the entrance of the pores and entrap DOX. On the other hand, Gd-based bovine serum albumin (BSA-Gd) complex was also demonstrated to entrap DOX within MSN mesopores, through the disulfide linkage [76]. Efficient *in vivo* cancer theranostics was achieved, with Gd as MRI contrast agent, redox-responsive cancer therapy and externally functionalized HA for cancer targeting.

Other than disulfide, coordination compounds which are also sensitive to the reducing tumor microenvironment could be utilized for redox-responsive drug delivery. Chen and co-workers designed RGD-functionalized magnetic redox-responsive MSN nanocarriers with the use of a Pt(IV) pro-drug as a redox-sensitive linker between MSN and pore-capping β-cyclodextrin [36]. After being exposed to the redox environment, Pt(IV) prodrug is transformed into active form - Pt(II) drug, which also releases the pore-loaded DOX for efficient cancer-targeted therapy. Magnetically enhanced accumulation of magnetic MSN and high contrast MRI for mapping tumor tissue were also demonstrated *in vivo*.

MSNs of small diameter (80 nm), with large pore size (5–10 nm) and pore volumes (2.3 $cm^3\ g^{-1}$), exhibiting fast biodegradation rate (releasing >81% of its Si content within 9 days in simulated body fluid) were recently applied as a multifunctional nanoplatform for combination immunotherapy and PET imaging [47]. Biodegradable MSNs (bMSNs, Fig. 3) contained radioisotope ^{64}Cu for PET imaging along with loaded CpG oligodeoxynucleotide adjuvant (CpG ODN) and photosensitizer Ce6 for synergistic PDT–immunotherapy. The as-synthesized bMSNs were PEGylated and conjugated with neoantigen peptides (ADP-dependent glucokinase, Adpgk) on the surface of MSNs through disulfide linkers that are easily cleavable in the highly reductive environment of tumors for antigen delivery. PET imaging confirmed the accumulation of prepared nanoconstructs in tumors, while employment of PDT with laser irradiation engaged dendritic cells to specific tumor sites to induce the production of antigen-specific, tumor-infiltrating cytotoxic T-lymphocytes for efficient PDT-enhanced personalized immunotherapy.

2.5. Enzyme-responsive MSN-based targeted cancer theranostics

Studies investigating enzyme-responsiveness of MSN-based nanomaterials for targeted cancer therapy use different overexpressed or increasingly active enzymes, to stimulate therapeutic activity at the tumor site [162]. For example, organotin-based metallodrug has been covalently attached to the MSNs surface through GFLG tetrapeptide linker [163], which is highly sensitive to the lysosomal cysteine protease cathepsin B that is overexpressed in breast adenocarcinoma. The material was also functionalized with FA for cancer-targeting and the material showed high *in vitro* activity, while *in vivo* studies demonstrated

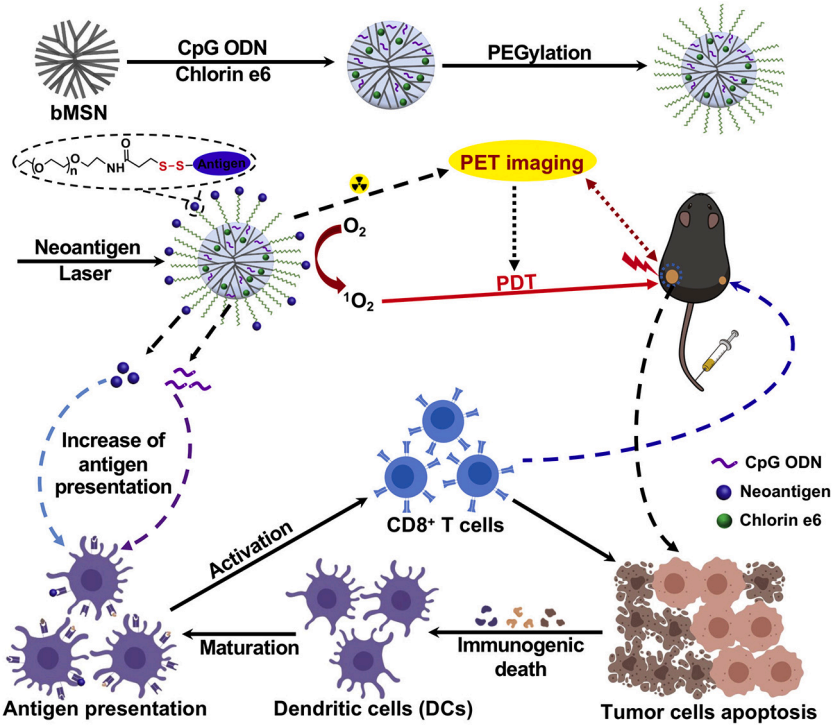

Fig. 3. Schematic representation of the synthesis of the nanoconstruct and its application for PDT-induced immunotherapy. Reproduced with permission [47].

preferential accumulation in tumor tissues and potent reduction of tumor size. Alternatively, Vaghasiya et al. incorporated collagen coating for controlling the release of Cisplatin (Cis) from MSNs in response to overexpressed MMP-2 [164]. A 2.4-fold higher amount of Cis was released when MMP-2 was present, implying good responsiveness and efficient capping capacity of the designed system. In a recent study, MSNs were functionalized with triphenylphosphine (TPP), a mitochondria-targeting compound, while DOX was encapsulated by the addition of HA, which endowed MSNs with pore sealing and targeting capability, as well as sensitivity to cancer-overexpressed hyaluronidase (HAase) [165]. The material was demonstrated to efficiently target mitochondria and preferentially deliver DOX to cancer cells. Dual enzyme-responsive DDS was also reported, such as in the case of fluorescence doped MSNs (FMSN), shelled with HA and collagen I, which are degraded by MMP-2 and HAase in tumor cells to release DOX [166].

When considering the nanosystems constructed for simultaneous therapy and imaging, a recent study reported MMP-2-responsive drug delivery based on the core/shell Fe_3O_4@MSN nanoplatform modified with a peptide PLGVR substrate [43]. In addition to the enzyme-responsive DOX delivery upon reaching the cancer tissue, magnet-guided composite accumulation in the tumors was demonstrated *in vivo*, while the presence of Fe_3O_4 allowed enhanced capabilities for T2-weighted MRI of cancer.

In another work, the authors dealt with constructing a novel tumor-targeting nanoplatform with dual imaging properties and PDT/chemo therapy [167]. Aminated MSN was first loaded with tirapazamine (TPZ) anticancer drug followed by a layer-by-layer alternating deposition of the negatively charged per-*O*-methyl-β-cyclodextrin-grafted-hyaluronic acid (HA-CD) and $TPPS_4$ (porphyrin derivative) that eventually formed CD-TPPS4 supramolecular photosensitizers (supraPSs), Fig. 4. In order to introduce MRI modality, Gd^{3+} was chelated to TPPS4 giving the final multilayer-coated MSN-based theranostic nanoplatform TPZ@MCMSN-Gd^{3+}. Active targeting is achieved with overexpressed CD44 receptor and upregulated HAase activity that triggers the release of TPZ and supraPSs.

A nanocomposite based on MSNs loaded with DOX, functionalized with aminopropyl groups, gated with negatively charged MUC1 aptamer for breast cancer controlled drug delivery and modified with ^{99m}Tc radioisotope for SPECT imaging was also reported [61]. The NPs managed to deliver DOX preferentially to tumor cells with the activity of DNAse I, while *in vivo* targeting ability and biodistribution of NPs were determined through SPECT imaging.

2.6. Light-responsive systems based on MSN with simultaneous imaging

Different recent reports describe the use of UV, visible or infrared irradiation to initiate the cancer treatment [143,168–170]. NIR light, which has higher tissue penetration capabilities than the light of lower wavelength, has been also applied to induce NIR-sensitive delivery of DOX and curcumin from mesoporous silica-coated $Cu_{1.8}S$ nanovehicle [37]. DNA hybrid helix was utilized as a sealing agent and controllable switch, allowing the cargo release due to its thermally-induced degradation, whereas conjugation with the aptamer enriched the system with targeting ability and improved cell membrane penetration. Photothermal (PT) performances of $Cu_{1.8}S$ NPs were also utilized for tumor-bearing Balb/c mice *in vivo* imaging. Thermosensitive liposomes have also been proposed for NIR irradiation-responsive cargo delivery. In their research, Sun et al. conjugated indocyanine green (ICG) and DOX-loaded/FA-modified thermosensitive liposomes onto the Gd-doped MSNs [52]. The complex design of nanoplatform was intended to accomplish chemo- and phototherapy of cancer, as well as diagnosis through triple-modal imaging. Efficient tumor shrinkage was noted by *in*

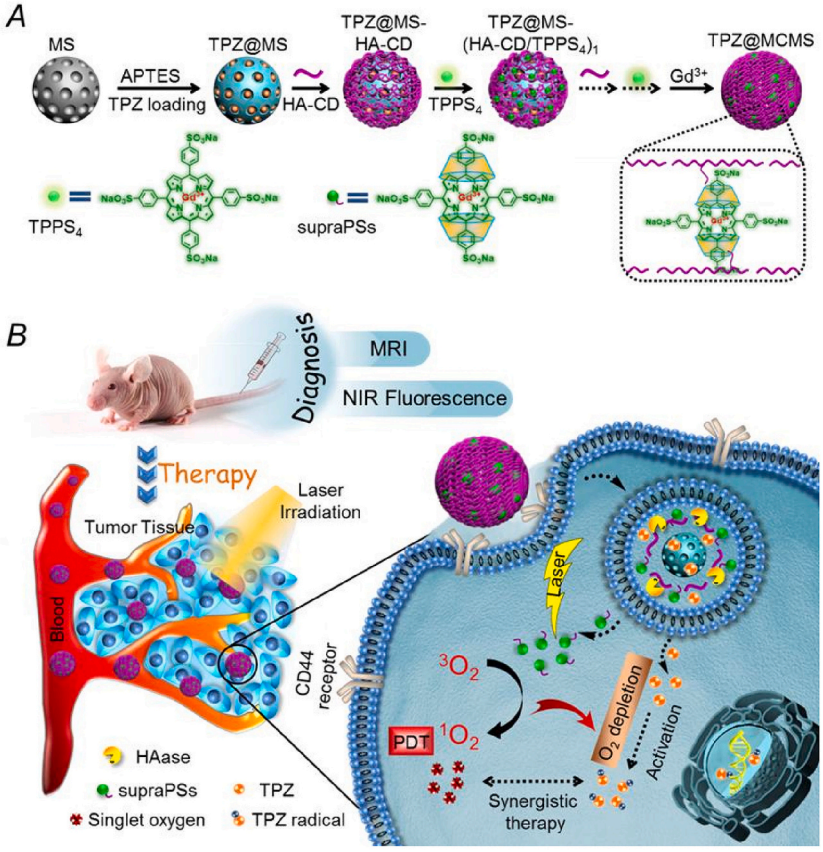

Fig. 4. Schematic representation of the construction, composition and theranostic applications of the nanomaterial for dual imaging (NIR fluorescence and MRI) and dual therapy (Chemotherapy and PDT). Reproduced with permission [167].

vivo experiments upon NIR laser-triggered controllable programmed synergistic chemo- and photo-therapy. In imaging modalities, ICG contributes to near infrared fluorescence (NIRF) imaging as well as photoacoustic (PA) imaging, whereas Gd ensured MRI functionality. Croissant et al. constructed MSN-based two photon-responsive nanocarrier by co-condensation of silylated two-photon electron donor (2PS) and silica precursor, subsequently loaded with DOX and capped with *bis*(propyl) disulfide moiety, while two-photon responsivity endowed the material with theranostic feature [38].

In the study by Wang et al., biocompatible periodic mesoporous organosilica coated with Prussian blue NPs (PB@PMOs) were synthesized for the loading of a biocompatible prodrug 5-aminolevulinic acid (5-ALA), to give PB@PMO-5-ALA for the treatment of glioma [70]. In malignant cells, 5-ALA is converted to protoporphyrin IX (PpIX), a powerful photosensitizer that can further trigger the photosensitive effect. PB exhibits catalytic ability to transform H_2O_2 to O_2 which is beneficial for PDT, and moreover, as PB contains iron ions, it was utilized for T2-weighted MRI. Porous core/shell Fe_3O_4@$mSiO_2$ containing upconversion NPs within the pores were also employed for simultaneous PTT and PDT upon excitation at 808 nm *in vivo* [171]. The as-synthesized platform exhibited magnetic-responsive cancer-targeting and strong PA and upconversion luminescence (UCL) signals. Yang et al. developed a nanoplatform consisting of rodlike mesoporous silica-coated with gold nanoshells (MSNR@Au hybrid) and further modified with ultrasmall gadolinium (Gd)-chelated supramolecular photosensitizers for *in vivo* quadmodal NIR fluorescence/MSOT/CT/MRI and NIR activated image-guided synergistic PTT/PDT anticancer therapy [172]. Two types of NIR-activatable, all-in-one lanthanide-doped mesoporous silica frameworks were developed by incorporating Eu/Gd oxide NPs [75]. The nanoconstructs were demonstrated for simultaneous bimodal fluorescence and T1-MRI, as well as for NIR light-triggered dual therapeutic functions (DOX delivery/release and nanomaterial-mediated PDT). It was also found that EuGdOx@MSF-mediated PDT effect suppresses the level of the P-glycoprotein (P-gp), which is associated with many cancers resistant to therapy.

The work by Goel et al. reported on Zr-89 radiolabeled hollow mesoporous silica (HMSN) with filled meso-tetrakis(4-carboxyphenyl) porphyrin (TCPP) within the pores, whereas the exterior was decorated with CuS NPs, aimed for application in effective multimodal cancer imaging and therapy [173]. TCPP is a hydrophobic molecule exerting intrinsic fluorescence (FL) and the capability to couple with radionuclides through the Cherenkov radiation energy transfer (CRET) phenomenon, while CuS nanocrystals show high capabilities for PTT. The resulting HMSNs integrate PET/FL/CL/CRET imaging on-demand for image-guided therapy *in vivo*, whereas enhanced hyperthermia and ROS production make this nanoconstruct suitable for synergistic PTT and PDT, along with chemotherapy through the loaded DOX. Experiments on mice bearing 4 T1 murine breast tumors injected with the constructed material showed prolonged blood retention, enhanced tumor accumulation, minimal systemic toxicity and complete tumor elimination within a day of treatment.

Huang et al. reported on improving PDT capabilities in hypoxic tumor tissues through exploiting high endogenous H_2O_2 concentrations in cancer cells and exposing the tumor environment to catalase for producing oxygen for PDT [174]. The authors constructed monodisperse dendritic mesoporous organosilica nanoparticles (MONs) with large

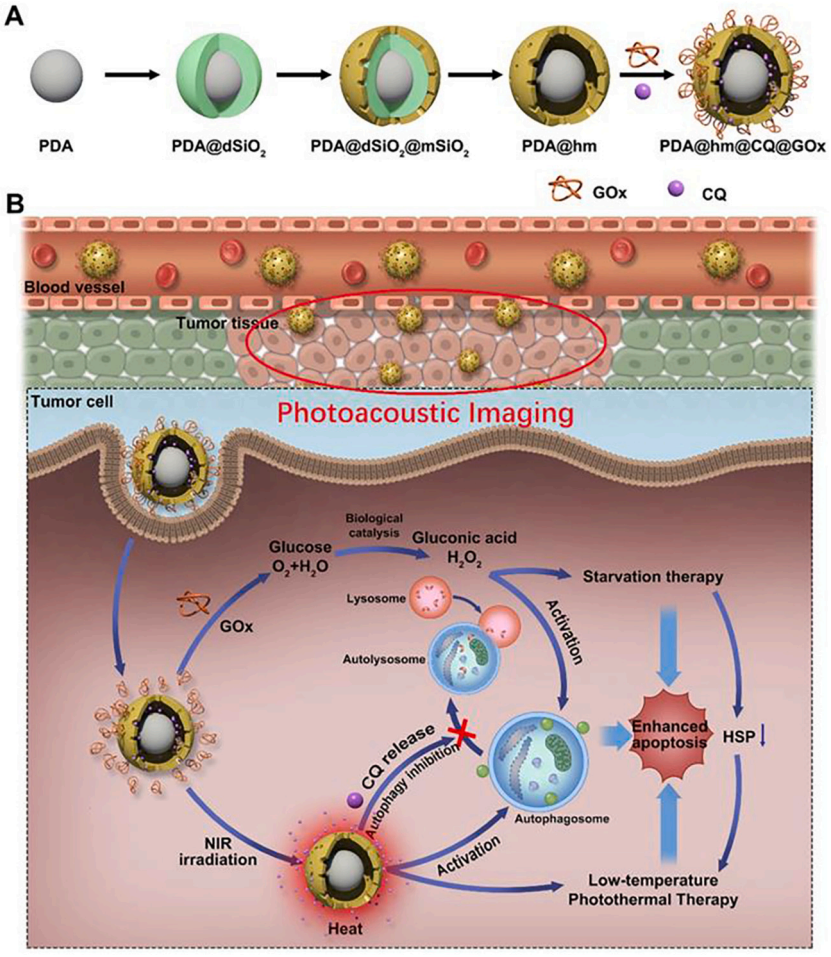

Fig. 5. Schematic representation for synthesis and application of the nanomaterial in simultaneous PA imaging and PTT. Reproduced with permission [175].

pore sizes of 15.9 nm, followed by loading ICG and catalase to give ICG-CAT@MONs for PA/US dual-modality image-guided PDT of cancer. Rattle-structured NPs with core PDA and hollow mesoporous silica as the shell (PDA@hm), were constructed for *in vivo* PA imaging and augmented low-temperature PTT through inhibiting expression of heat shock proteins (HSPs) by glucose depletion and simultaneous inhibition of autophagy (Fig. 5) [175]. The central cavity of PDA@hm was used to load autophagy-inhibitor drug chloroquine (CQ), while glucose oxidase (GOx) was conjugated onto the surface of the mesoporous silica shell making a corona-like structure. *In vitro* and *in vivo* assessment upon exposure to 808 nm laser showed efficient PA imaging capabilities of PDA@hm@CQ@GOx, while increased cell apoptosis could be observed, indicating the pro-apoptotic effect of the nanoconstructs for low-temperature PTT, upon simultaneous cancer starvation and inhibition of autophagy.

In another study, PDA-decorated MSN–based nanotheranostic platform was developed with an internal cavity containing perfluorohexane (PFH), ICG as NIR photosensitizer embedded within the PDA layer, and PEG-folate (FA) for cancer-targeting to give MSNs-PFH@PDA-ICG-PEG-FA [176]. This nanoplatform exhibits ultrasonic (US)/NIRF dual imaging that enables image-guided PTT and PDT combination therapy. In more detail, the PDA layer blocks the release of the encapsulated PFH while ICG, upon 808 nm NIR irradiation, triggers the formation of ROS and hyperthermia, which in turn opens the pores of MSNs and induces PFH phase transformation from liquid to gas. Consequently, this causes the formation of large bubbles exploited for US imaging. *In vivo* PTT/PDT combination therapy confirmed tumor growth inhibition and complete curing in three out of five mice, without toxic side effects.

2.7. MSN-based magnetic field responsive cancer theranostics

Different core/shell analogues of MSNs can be constructed containing magnetic (typically SPION) NPs as cores, which augment the properties of MSNs with capabilities for magnetic-responsive targeting of cancer, triggering drug delivery in response to magnetic field and possibilities to act as a contrast agent in T2-weighted MRI, which were recently reviewed in detail [24]. The surface of magnetic MSNs is typically functionalized with engineered thermosensitive polymers. Upon employing an alternating magnetic field (AMF) local temperature increases due to Néel and Brownian relaxation of SPION, which causes polymer shrinkage [177] or breakage [178], leading to the release of cargo molecules.

Perton et al. developed magnetic core/shell nanocomposites with magnetic hyperthermia and MRI properties [179]. Carboxylated CdSe/ZnS QDs were grafted inside the pores of large pore stellate mesoporous silica (STMS) shell for fluorescence imaging. Surface modification with isobutyramide enabled tight binding of human serum albumin, which ensures biocompatibility and increased presence of the NPs in blood circulation. Synergistic effects of magnetic hyperthermia at low frequency and amplitude field (100 kHz, 117 G or 9.3 kA m^{-1}), and DOX delivery were demonstrated to lead to efficient cancer cell death, in addition to capabilities for bimodal MRI and fluorescence imaging.

Core/shell magnetic MSN-based nanosystem was also designed, capable of delivering the anticancer drug TPZ inside the nucleus of cancer stem cells (CSCs) owing to magnetic hyperthermia-triggered drug release [180]. The nanosystem structure consisted of four layers: superparamagnetic iron oxide NPs core, mesoporous silica shell, nucleus-targeting agent TAT peptide, and a thermo-sensitive azo linker conjugated antibody (anti-CD133). Such a structure enabled Fe_3O_4 NPs core to generate heat under AMF, which breaks the thermo-sensitive bond and further leads to exposure of TAT peptide for CSCs-nucleus targeting and finally induces MSN-loaded TPZ release. It has been demonstrated that thermal-triggered drug release significantly reduced the premature release in endosomes and lysosomes compared to pH-responsive drug release, and enhanced the accumulation of the drug in the cell nucleus.

A novel nanosystem composed of a self-healing hydrogel based on natural polymers – benzaldehyde functionalized pullulan and amino containing PEG-modified chitosan, containing Rhodamine B isothiocyanate -labeled/mesoporous silica-coated $Mn_{0.6}Zn_{0.4}Fe_2O_4$ nanospheres for MRI and magnetothermal-chemo-chemodynamic therapy was recently reported [181]. Unlike the use of conventional Fe_3O_4 based NPs as T2-contrast agents, Mn^{2+} and Zn^{2+} doped ferrite NPs exhibit higher SAR (specific absorption rate, conversion efficiency from electromagnetic energy into heat energy under AMF) and can show catalase-like activity. The tumor microenvironment is acidic and high in H_2O_2 concentration, where these particles can induce Fenton-like reactions and generate toxic $^{\bullet}OH$ radicals. Exposure to AMF leads to magnetic hyperthermia and remarkable anticancer effects both *in vitro* and *in vivo* on 4 T1 tumor cells.

2.8. Ultrasound-responsive MSN-based delivery systems and simultaneous imaging

In order to achieve the US-responsiveness of MSNs, Paris et al. modified its surface with the copolymer containing US-sensitive hydrophobic tetrahydropyranyl (THP) monomers [182]. The loading and release principle is based on the conformational changes and US cleavage of tetrahydropyranyl monomers. Namely, cargo is loaded at 4 °C and trapped at physiological temperature due to the conformational changes from coil-like to a collapsed state. Upon US exposure and cleavage of mentioned moieties the polymer becomes more hydrophobic, leading to coil-like conformation and pores opening, *i.e.* the cargo release.

Cheng et al. employed high intensity focused US (HIFU) to stimulate Gd-based cargo ($Gd(DTPA)^{2-}$) release from PEG-coated MSN nanocarrier [183]. The integration of PEG moiety blocked the entrance and enabled the opening of the pores due to HIFU induced polymer vibration and/or bond cleavage. The released amount of cargo could be adjusted by changing HIFU power levels and exposure time. These results were obtained by tracking $Gd(DTPA)^{2-}$ release in *ex vivo* chicken breast tissue samples by MRI.

An interesting approach was obtained through designing so-called "cell bombs", by loading DOX and phase transformable perfluoropentane (PFP) into hollow mesoporous organosilica nanoparticles (HMONs), followed by their internalization into macrophages. Drug release was based on PFP HIFU-induced evaporation, subsequent mild hyperthermia and disruption of macrophages, which leads to DOX release [39]. Evaporation-induced bubbles generation produced an echo signal, which was further exploited for real-time tracking of constructed cell bombs and higher DOX amount was released in tumor cells in case of HIFU exposure. Eventually, the treatment of tumor tissues in mice with the combination of cell bombs and sonication inhibited the tumor growth, but more significantly, kept the mice alive 28 days longer. US-responsive PEGylated mesoporous silica-titania nanocarrier was also constructed having a therapeutic mechanism based on ROS generation by PFH, encapsulated gas precursor, due to US-induced cavitation [62]. Also, ROS generation was enhanced owing to efficient energy transfer to titania, resulting in improved antitumor therapy. Furthermore, PFH enabled prolonged PA imaging since its rapid vaporization gave a strong PA signal after 6 h.

The study by Huang et al. reports on the fabrication of a high-performance multifunctional nanoparticulate sonosensitizer based on a mesoporous organosilica nanosystem for efficient *in vivo* MRI-guided sonodynamic therapy (SDT) for cancer treatment [74]. HMONs with disulfide bonds (S-S), responsive to the reductive tumor microenvironment, hybridized into the framework were developed as nanocarriers for the covalent attachment of the sonosensitizer protoporphyrin (PpIX). In order to obtain a T1-weighted MR imaging modality, paramagnetic manganese ions (Mn) were chelated into the porphyrin ring (HMONs-MnPpIX). *In vitro* tests on 4 T1 cells, as well as *in vivo* evaluations performed on 4 T1 cell-bearing mice demonstrated high SDT efficiency for

inducing cancer cell death and suppressing the tumor growth under US irradiation, while achieving high T1-weighted positive MRI contrast of the tumor region.

Usage of interfacial nanobubbles (INBs) on superhydrophobic surfaces as solid cavitation agents (Fig. 6) for US contrast imaging enhancement as well as for chemo-sonodynamic therapy was recently reported [184]. Multifunctional MSNs were loaded with DOX and designed to contain superhydrophobic fluorocarbon-modified surface and capping amphiphilic β-cyclodextrin moieties. Upon US exposure, INBs area accumulated at the interface of hydrophobic MSN surface, which subsequently enables anti-vascular therapy by mechanical force, along with simultaneous ROS generation for sonodynamic therapy and DOX release for chemotherapy. Repeated *in vivo* INB cavitation was demonstrated by single-injection FMSNs-DOX with multiple US sonication, demonstrating potent tumor growth inhibition along with simultaneous US imaging.

Core/shell magnetic MSN for MRI-guided high-intensity focused US-responsive spatiotemporal drug delivery was also developed containing SPION core doped with manganese and cobalt for improving its T2 contrast enhancement [185]. The chemotherapeutic DOX was capped with a HIFU-responsive aliphatic azo-containing compound, 4,4′-azobis (4-cyanovaleric acid) (ACVA). HIFU irradiation irreversibly cleaves covalent C-N bonds of ACVA, enabling pore opening and drug release. Cellular experiments examined on human pancreatic cancer cells, PANC-1, showed therapeutic efficacy as a result of increased amounts of the released drug, self-reported by the associated MRI contrast change.

2.9. Dual- and multi-stimuli responsive MSNs with simultaneous imaging

As MSN surface can be selectively modified, typically with one type of functionalization on the external surface and another within the mesopores, possibilities exist for designing theranostics for combination cancer therapy [186,187]. Thus, cancer targeting may be enhanced in case of controlling the therapeutic activity in response to multiple cancer-specific stimuli, while combining different modes of therapy may circumvent the occurrence of drug resistance and enhance the therapeutic efficacy. Chemo/PT therapeutic mesoporous silica-coated mesoporous carbon nanocomposite (MCN@Si) with multi-stimuli responsive behavior was fabricated by Lu and co-workers [41]. Carbon dots (CDs) as gatekeepers were covalently bonded on the surface of MCN@Si through disulfide bonds, and anticancer drug DOX was encapsulated inside the dual-porous system, which enhanced drug loading capacity. Exposure to weakly acidic pH, presence of GSH and NIR irradiation have been demonstrated to induce synergistic therapeutic effects against cancer cells *in vitro* and *in vivo*.

Wan et al. reported on dual-responsive MSN-based nanoplatform intended for diagnosis and cancer treatment based on core/shell magnetic MSNs with core-Fe_3O_4 as an MRI contrast agent [42]. MSN pores were loaded with DOX and capped with branched polyethyleneimine (PEI) *via* disulfide bonds. PEI was further coupled with citraconic anhydride for precise targeting and increased biocompatibility. The amino groups of PEI are blocked by citraconic anhydride, thereby reversing the positive surface charge responsible for cytotoxicity and non-specific interactions with negatively charged serum albumin [188]. Controlled drug delivery was established dually, due to PEI charge conversion in response to acidic pH and redox responsiveness of a disulfide linkage.

In the article by Fang et al. a dual-stimuli responsive (pH change and NIR light irradiation) nanotheranostic platform composed of mesoporous silica-coated gold nanorods (GNR@SiO_2) was synthesized containing functionalized ICG for fluorescence imaging and PDT, and pore-loaded drug 5-fluorouracil (5-FU), for *in vivo* multimodal image-guided synergistic PTT, PDT and chemotherapy [57]. Image-guided PT-chemotherapy strategy for the highly aggressive triple negative breast cancer (TNBC) was developed by coating PB NPs with periodic mesoporous organosilica (PMO) shell [189]. PB NPs, due to their absorbance in the NIR region, high PT conversion efficiency and T1-weighted

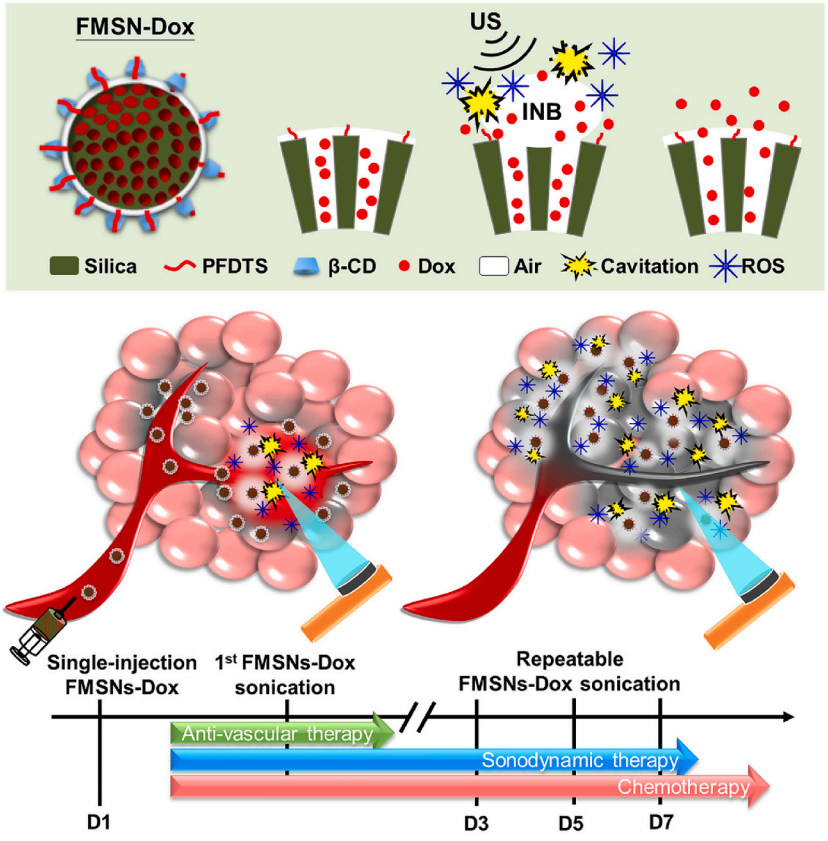

Fig. 6. Interfacial nanobubbles (INBs) are accumulated at the superhydrophobic surface of FMSNs-DOX upon US exposure to induce bubble cavitation, ROS generation, and drug release. Enhanced accumulation of FMSNs-DOX within tumor tissue was achieved upon single-injection FMSNs-DOX and subsequent INB cavitation to produce anti-vascular effect. Repeated exposure to US allows additional therapy modalities, such as sonodynamic therapy and chemotherapy. Reproduced with permission [184].

contrasting ability, can be used for PA imaging, PTT and MRI. The combined PTT and chemotherapy effectively inhibited TNBC in the MDA-MB-231-Luc tumor-bearing mouse, by inducing cell apoptosis and necrosis in the tumor region, without harmful effects on major organs.

3. MSNs for gene editing in cancer treatments

Cancer gene therapy is based on the transfer of genes directly into the cancer cells or alternatively into the tissue surrounding the tumor. The goal of such therapy is to affect the abnormal genes in the cancer cells, either by regulation or replacement, and ultimately cause the death of the cancer cells either directly or *via* preventing the tumor neovascularization which should deprive the tumor cells of nutrients and cause them to die.

Therapeutic genetic material can be oligonucleotides of DNA (such as plasmid DNA (pDNA) and minicircle DNA (mcDNA)), RNA oligonucleotides (such as small interfering RNA (siRNA), micro RNA (miRNA), messenger RNA (mRNA)) [190,191], and increasingly nucleic acid aptamers [192] and CRISPR/Cas9 nuclease system [193]. However, as therapeutic genetic material would get quickly degraded by serum endonucleases and RNAses [194], effective gene delivery systems are needed to protect the genetic material as well as to enable it to reach the nucleus of the cell, over the physiological, extra- and intracellular barriers [195].

There is a number of excellent reviews addressing the various viral and non-viral gene delivery vectors used in cancer gene therapy. More specifically, we draw the readers' attention to recent reviews on silica-based gene delivery systems [196] and on MSNs for co-delivery of drugs and nucleic acids in oncology [197]. Herein we opted to cover a specific topic, namely MSNs for CRISPR/Cas9 systems delivery and gene editing, which is quite novel but also highly attractive research field as the Nobel Prize in Chemistry in 2020 was awarded to Emmanuelle Charpentier and Jennifer A. Doudna for the development of CRISPR/Cas9 methodology.

In general, MSNs are proving to be a good candidate for the delivery of therapeutic genetic material as the surface of MSNs can be modified to have net positive charges, *e.g.* by amination or cationic polymer functionalization [198], which can further increase adsorption of the negatively charged nucleic acid molecules and enable the so-called "proton sponge effect" to facilitate the escape of MSNs from endosomes/lisosomes [199].

3.1. MSNs for CRISPR/Cas9 systems delivery

Clustered regularly interspaced short palindromic repeat-CRISPR-associated protein (CRISPR-Cas) is a method for genome editing that has been developed in the recent years and led to the Nobel Prize in Chemistry in 2020. The method exploits the prokaryotic adaptive immune system.

There are two classes of CRISPR systems: Class 1 systems that utilize a complex of multi-Cas proteins and Class 2 which uses a single large Cas protein [200,201]. Each class has different types (Class 1 - Types I, III and IV, and Class 2 - Types II, V and VI). Type II CRISPR/Cas9 system is currently the main protein used for genome editing [202].

The type II CRISPR/Cas9 system is made of Cas9 endonuclease and guideRNA (gRNA) with its customizable component CRISPR RNA (crRNA) that enables specificity, *i.e.* binding to the specific DNA sequence. The system also contains a constant trans-activating crRNA (tracrRNA) [203]. Cas9 forms a ribonucleoprotein (RNP) complex with crRNA and tracrRNA, and this complex cleaves double-stranded DNA at the targeted sequence *via* crRNA matching.

In the artificial systems and particularly important for the cancer applications, crRNA and tracrRNA can be transformed into synthetic single guide RNA (sgRNA) that functions as a guiding element and can direct Cas9 protein to generate site-specific double-stranded DNA breaks in any targeted genomic locus containing appropriate motif, *i.e.* protospacer-adjacent motif (PAM) [204]. sgRNA-mediated reprogramming of Cas9 allows targeting of several target gene sequences at the same time, which gives unparalleled opportunities for investigation of cancer-associated genes [205,206].

Furthermore, the genes can be regulated by utilizing the CRISPR in combination with the nuclease-deficient dCas9 which is specifically designed not to generate DNA cleavages, but to very precisely bind DNA when guided by sgRNA [206]. Such CRISPR-dCas9 systems show great potential for cancer therapy. Rahman and Tollefsbol show that when CRISPR-dCas9 is ligated to the epigenetic effectors. it forms the complexes that can perform epigenetic editing and consequently change the cancerous epigenetic features [207].

However, there are several technical aspects that render application of the "naked" CRISPR-(d)Cas9 systems difficult: 1) "Naked" CRISPR-Cas9 complexes are prone to degradation by serum nucleases, 2) can activate innate immune system, 3) can exert non-specific action on non-target cells and serum proteins, 4) do not enter target tissues from the blood vessels, and 5) can be cleared out by the renal system before entering the target tissues [208]. These need to be mitigated by efficient delivery strategies [208,209]. Various designs and methods of delivery are being investigated such as viral vectors, physical methods like electroporation, mechanical cell deformation *etc.*, but the nanocarriers have been showing the greatest potential for several reasons. First of all, nanocarriers, similar to most other types of non-viral vectors, provide low immunogenicity, can be produced in a relatively easy way, can encapsulate significant amounts of therapeutic genetic material and importantly, can be functionalized with targeting molecules enabling the specific, targeted delivery of the genetic cargo. On the other side, the efficiency of the genetic cargo delivery by nanocarriers is still low in comparison with the viral vectors. This implies that nanocarriers should be further optimized. Rigid nanocarriers such as carbon and inorganic NPs are particularly well suited for further optimization due to their controllable features such as a high surface area to volume ratio, tunable size, surface functionalization and high stability in physiological environments [208,209]. However, one should always consider the toxicity of the nanocarriers. For example, gold and polymer NPs, and some lipid-based nanocarriers exert dose-dependent toxicity and have lower delivery efficiency when compared to other nanocarriers with a greater surface area such as silica-based ones [210].

Noureddine et al. used modified monosized lipid-coated MSNs (LC-MSNs) for loading of CRISPR components (145 μg ribonucleoprotein RNP *i.e.* cas9-sgRNA complex or 40 μg plasmid pCRISPR *i.e.* expression vector for Cas9 and sgRNA per mg of MSNs) and release within HeLa cervical and A549 lung cancer cells [193]. Both options exerted good compatibility with both cell types, while pCRISPR@LC-MSN achieved modest effects in HeLa in comparison to A549 cells. The study showcases the potential of the carrier system (Fig. 7) composed of lipid-coated MSNs for CRISPR-components delivery in the cancer cells, although the achieved editing efficiency is still subpar, particularly for the plasmid pCRISPR-loaded NPs which showed negative results in terms of gene editing, probably due to the size of the plasmid. However, the RNP-loaded MSNs achieved editing of up to 10% in reporter cancer cells *in vitro* with more than 70% release of RNP from NPs within 72 h.

MSNs modified to the state of "virus-like nanoparticle - VLN" were used by Liu et al. for co-delivery of CRISPR/Cas9 system and small molecule drugs for the treatment of malignant tumors [211]. VLNs had a core/shell structure, in which small molecule drug (axitinib) and CRISPR/Cas9 system (with sgRNA-targeting programmed death-ligand 1 -PD-L1) are loaded in the MSN-based core, which is further encapsulated with a lipid shell. Such structure allows VLN stability in blood circulation. The MSNs were surface-thiolated (MSN-SH), axitinib was loaded into the pores, which were then locked by conjugating the ribonucleoprotein RNP to MSN-SH *via* disulfide bonds. This construct was then encapsulated by a lipid layer containing PEG2000-DSPE in order to prolong the circulation time and protect RNP from enzymatic degradation in a physiological environment. When VLNs reach the

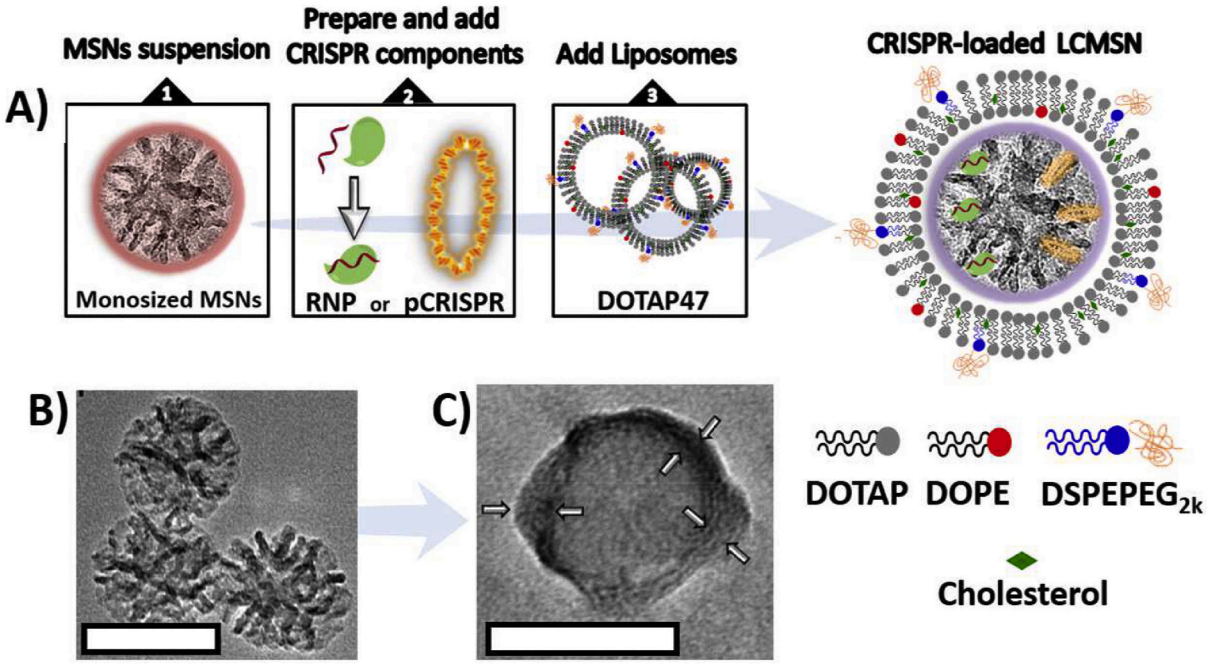

Fig. 7. Schematic showing the step by step formation of CRISPR-LC-MSN: (A) MSNs were suspended in water (1), followed by the addition of freshly complexed RNP or pCRISPR (2), then encapsulated *in situ* with positively charged liposomes to form CRISPR@LC-MSN (3). (B-C) TEM images of (B) surfactant-and lipid-free stellate MSNs; (C) RNP@LC-MSNs stained with phosphotungstic acid, arrows on the dark halo indicating lipid layers (scale bar = 100 nm). Reproduced with permission [193].

tumor and get internalized, the high concentration of glutathione in tumor cleaves the disulfide bond between RNP and MSN-SH, allowing the RNP to get delivered into the nuclei of the tumor cells for the PD-L1 targeted gene editing. This approach led to disruption of multiple immunosuppressive pathways and suppression of the growth of melanoma *in vivo*. This platform shows great promise for intravenous application and co-delivery of small molecule drugs and CRISPR-Cas9 system, however, similarly to the previously reviewed study by Noureddine

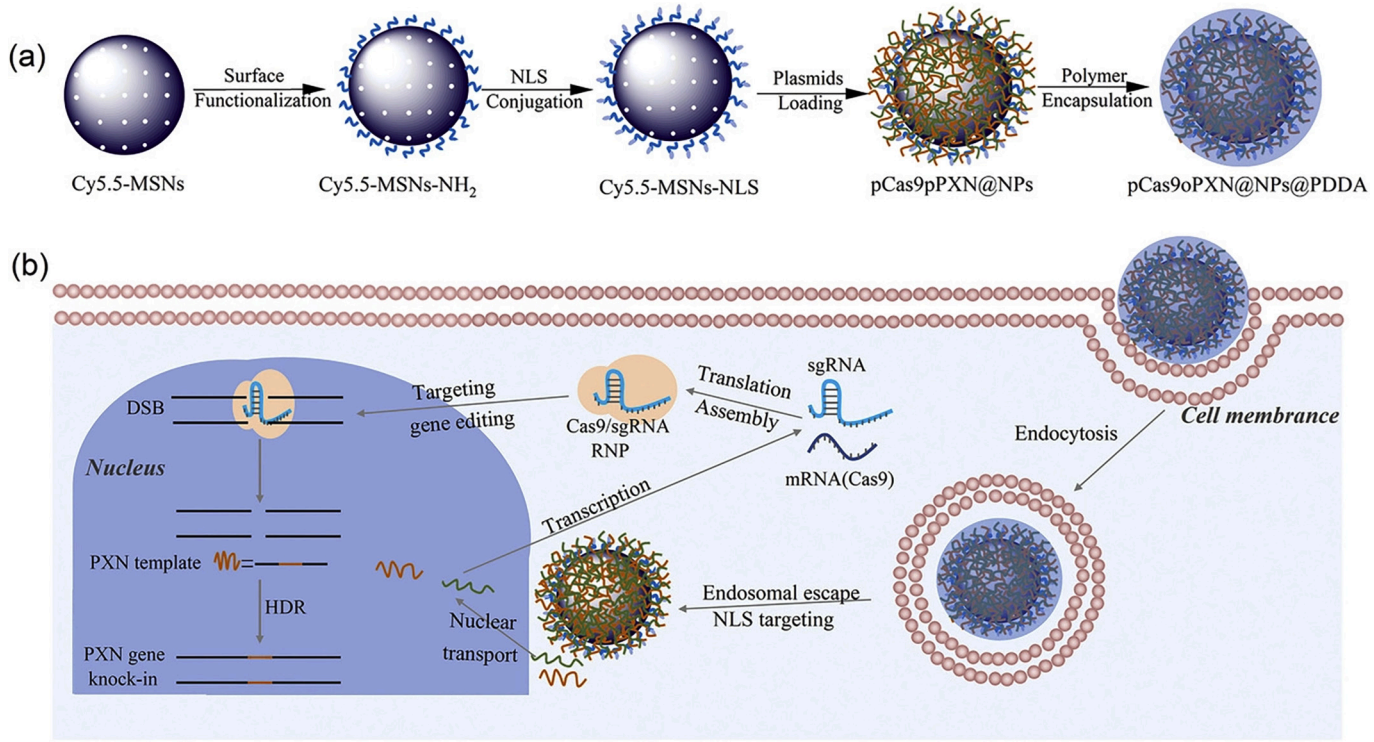

Fig. 8. Schematic illustration of the functionalized MSNs-based nanocarrier for the delivery of CRISPR/Cas9 plasmids: a) preparation of Cy5.5-MSNs-NLS, plasmid loading, and polymer encapsulation; b) intracellular delivery of the two kinds of plasmids to the nucleus for paxillin gene knock in. Reproduced with permission [212].

et al. there is still room for optimization of the VLN construct for more specific targeting to the tumor cells.

Xu et al. performed intracellular delivery of CRISPR/Cas9 plasmids by polymer-coated MSNs, functionalized with a fluorescent dye (Cy5.5) and the surface was conjugated with nuclear localization sequence (NLS), exhibiting high loading efficiency toward the paxillin (PXN) cutdown plasmid, GFP-Cas9-paxillin_gRNA and repair plasmid [212]. Paxillin family members have been linked to malignant cancer progression, particularly in lung, breast and prostate tumors [213]. Polymer coating consisted of poly(dimethyldiallylammonium chloride) (PDDA) and was deposited onto MSNs by microfluidic nanoprecipitation. The coating showed good protection against denaturation and prevented premature release. In addition, it was observed that due to the positive charge and pH-responsive disaggregation of PDDA, coated MSNs achieved enhanced cellular internalization (16 h) and endosomal escape (4 h). After achieving escape to the cytoplasm, the NLS from the nanoparticle surface facilitates nuclear transport of the CRISPR/Cas9 plasmids leading to the successful GFP-tag knock-in of the PXN genomic sequence in human bone osteosarcoma epithelial cells (U2OS) cells (Fig. 8). Intracellular localization of the Cy5.5-labeled MSNs as well as the efficacy of the GFP knock-in transfection were visualized by fluorescence microscopy.

As evidenced in the discussed studies, there is still an issue of targeting MSNs carrying genetic material to the specific cells. In a recent study, Ma et al. implemented CRISPR-dCas9 for the guidance of the MSNs into nuclei in combination with a telomerase-responsive nanosystem for tumor-specific release of DOX [214]. The authors used sgRNA that targets telomere-repetitive sequences at the ends of chromosomes, in combination with a nuclease-deficient dCas9 protein. This enabled specific targeting of the CRISPR-dCas9/MSN constructs to the nucleus. In addition, they also achieved telomerase-mediated release of DOX from MSNs, by adding a specific wrapping DNA on the dCas9-MSN construct. The specific wrapping DNA gets extended in the presence of the overexpressed telomerase enzyme in the cancer cells. The used wrapping DNA is designed to have complementary 3′ and 5′ ends of the generated telomeric repeats, leading to the formation of a rigid hairpin-like DNA structure. The hairpin causes detachment of the wrapping DNA from the MSN surface and the release of DOX into the nucleus. The *in vitro* experiments in the HeLa cells indicated that DOX encapsulated in dCas9-MSNs/DOX/DNA was gradually released in the whole cell, and preferentially in the nucleus, during the period of 12–24 h post-transfection. The authors also evaluated the effects in HeLa tumor-bearing BALb/c mice and achieved 88% growth suppression at the end of treatments.

4. Conclusions and outlook

Characteristics of MSNs are highly suitable for designing complex multifunctional nanosystems for simultaneous cancer therapy and imaging. A range of possibilities exist in devising nanotheranostics based on MSNs, with combinations of different treatment modalities, such as drug delivery in response to cancer-characteristic weakly acidic extracellular environment, to reductive intracellular conditions, or to the presence of overexpressed enzymes or receptors in tumors. External stimuli, applicable for localized cancer therapy, mainly include exposure to light, magnetic field and US, while their mechanism of action may involve triggering the release of cytotoxic drugs upon exposure to these stimuli or inducing the formation of reactive oxygen species (PDT or sonodynamic therapy) or heat (PTT or magnetic hyperthermia). Furthermore, MSNs offer a range of opportunities for devising nanosystems for gene therapy and editing.

Therapeutic approaches using MSNs are being efficiently combined with different imaging modalities through various types of surface functionalization, construction of core/shell nanomaterials and through the entrapment of cargo molecules within the pores. The range of imaging modalities employed includes: MRI (T1- and T2-weighted), PA, PT, NIRF and thermal imaging, PET, SPECT, CT (X-ray), sonography and MSOT. The theranostic capability, along with different possible morphologies and compositions of NPs, open virtually endless opportunities for the construction of multifunctional theranostic MSN-based nanosystems. Research on these multipurpose nanomaterials is expanding, and highly efficient novel theranostic nanomaterials have been proposed recently, demonstrating the richness and creativity of this research area and the high potential for future applications in image-guided and personalized therapies. However, despite the overwhelming advances, clinical trials of silica-based NPs for cancer treatment and imaging are substantially lagging behind the research. Therefore, it would be highly beneficial to stir future activities in this field of research, not necessarily toward designing increasingly complex nanotheranostics, but instead, focusing on the construction of MSN-based nanosystems with enhanced attractiveness for embarking on clinical trials and translation into clinical practice.

Declaration of competing interest

The authors declare no conflict of interest.

Acknowledgements

The authors would like to thank the Ministry of Education, Science and Technological Development of the Republic of Serbia (Grant No: 451-03-9/2021-14/200358), the Science Fund of the Republic of Serbia, PROMIS (PRECAST Grant No: 6060755) and European Union's Horizon 2020 research and innovation programme under grant agreement No. 952259 (NANOFACTS) and grant agreement No. 758887 (REACT) for financial support.

Received: ((will be filled in by the editorial staff)).
Revised: ((will be filled in by the editorial staff)).
Published online: ((will be filled in by the editorial staff)).

References

[1] S.D. Undevia, G. Gomez-Abuin, M.J. Ratain, Pharmacokinetic variability of anticancer agents, Nat. Rev. Cancer 5 (2005) 447–458, https://doi.org/10.1038/nrc1629.
[2] K.M. Sullivan, H.L. Kenerson, V.G. Pillarisetty, K.J. Riehle, R.S. Yeung, Precision oncology in liver cancer, Ann Transl Med. 6 (2018) 285, https://doi.org/10.21037/atm.2018.06.14.
[3] L. Palmerston Mendes, J. Pan, V.P. Torchilin, Dendrimers as nanocarriers for nucleic acid and drug delivery in cancer therapy, Molecules. 22 (2017) 1401.
[4] P. Yingchoncharoen, D.S. Kalinowski, D.R. Richardson, Lipid-based drug delivery systems in cancer therapy: what is available and what is yet to come, Pharmacol. Rev. 68 (2016) 701–787.
[5] J. Liu, J. Dong, T. Zhang, Q. Peng, Graphene-based nanomaterials and their potentials in advanced drug delivery and cancer therapy, J. Control. Release 286 (2018) 64–73.
[6] Y.H. Yun, B.K. Lee, K. Park, Controlled drug delivery: historical perspective for the next generation, J. Control. Release 219 (2015) 2–7.
[7] S. Mura, J. Nicolas, P. Couvreur, Stimuli-responsive nanocarriers for drug delivery, Nat. Mater. 12 (2013) 991–1003.
[8] L.C.S. Erthal, O.L. Gobbo, E. Ruiz-Hernandez, Biocompatible copolymer formulations to treat glioblastoma multiforme, Acta Biomater. 121 (2021) 89–102, https://doi.org/10.1016/j.actbio.2020.11.030.
[9] A.C. Anselmo, S. Mitragotri, Nanoparticles in the clinic, Bioeng. Transl. Med. 1 (2016) 10–29, https://doi.org/10.1002/btm2.10003.
[10] A.C. Anselmo, S. Mitragotri, Nanoparticles in the clinic: An update, Bioeng. Transl. Med. 4 (2019), https://doi.org/10.1002/btm2.10143 e10143–e10143.
[11] S. Senapati, A.K. Mahanta, S. Kumar, P. Maiti, Controlled drug delivery vehicles for cancer treatment and their performance, Signal Transduct. Target. Ther. 3 (2018) 7, https://doi.org/10.1038/s41392-017-0004-3.
[12] A. Raza, U. Hayat, T. Rasheed, M. Bilal, H.M.N. Iqbal, Redox-responsive nanocarriers as tumor-targeted drug delivery systems, Eur. J. Med. Chem. 157 (2018) 705–715, https://doi.org/10.1016/j.ejmech.2018.08.034.
[13] Z. Liao, S.W. Wong, H.L. Yeo, Y. Zhao, Smart nanocarriers for cancer treatment: Clinical impact and safety, NanoImpact. 20 (2020) 100253, https://doi.org/10.1016/j.impact.2020.100253.
[14] S. Wilhelm, A.J. Tavares, Q. Dai, S. Ohta, J. Audet, H.F. Dvorak, W.C.W. Chan, Analysis of nanoparticle delivery to tumours, Nat. Rev. Mater. 1 (2016) 16014, https://doi.org/10.1038/natrevmats.2016.14.
[15] X. Liu, P. Lin, I. Perrett, J. Lin, Y.P. Liao, C.H. Chang, J. Jiang, N. Wu, T. Donahue, Z. Wainberg, A.E. Nel, H. Meng, Tumor-penetrating peptide enhances transcytosis

of silicasome-based chemotherapy for pancreatic cancer, J. Clin. Invest. 127 (2017) 2007–2018, https://doi.org/10.1172/JCI92284.
[16] X. Liu, J. Jiang, R. Chan, Y. Ji, J. Lu, Y.P. Liao, M. Okene, J. Lin, P. Lin, C. H. Chang, X. Wang, I. Tang, E. Zheng, W. Qiu, Z.A. Wainberg, A.E. Nel, H. Meng, Improved efficacy and reduced toxicity using a custom-designed irinotecan-delivering silicasome for orthotopic colon cancer, ACS Nano 13 (2019) 38–53, https://doi.org/10.1021/acsnano.8b06164.
[17] S.D. Allen, X. Liu, J. Jiang, Y.P. Liao, C.H. Chang, A.E. Nel, H. Meng, Immune checkpoint inhibition in syngeneic mouse cancer models by a silicasome nanocarrier delivering a GSK3 inhibitor, Biomaterials. 269 (2021) 120635, https://doi.org/10.1016/j.biomaterials.2020.120635.
[18] X. Liu, J. Jiang, C.H. Chang, Y.P. Liao, J.J. Lodico, I. Tang, E. Zheng, W. Qiu, M. Lin, X. Wang, Y. Ji, K.C. Mei, A.E. Nel, H. Meng, Development of facile and versatile platinum drug delivering silicasome nanocarriers for efficient pancreatic cancer chemo-immunotherapy, Small. 17 (2021) 1–13, https://doi.org/10.1002/smll.202005993.
[19] X. Liu, J. Jiang, Y.P. Liao, I. Tang, E. Zheng, W. Qiu, M. Lin, X. Wang, Y. Ji, K. C. Mei, Q. Liu, C.H. Chang, Z.A. Wainberg, A.E. Nel, H. Meng, Combination chemo-immunotherapy for pancreatic cancer using the immunogenic effects of an irinotecan silicasome nanocarrier plus anti-PD-1, Adv. Sci. 8 (2021) 1–17, https://doi.org/10.1002/advs.202002147.
[20] R. Jugdaohsingh, Silicon and bone health, J. Nutr. Health Aging 11 (2007) 99–110.
[21] N.Ž. Knežević, E. Ruiz-Hernández, W.E. Hennink, M. Vallet-Regí, Magnetic mesoporous silica-based core/shell nanoparticles for biomedical applications, RSC Adv. 3 (2013) 9584, https://doi.org/10.1039/c3ra23127e.
[22] M. Martínez-Carmona, Q.P. Ho, J. Morand, A. García, E. Ortega, L.C.S. Erthal, E. Ruiz-Hernandez, M.D. Santana, J. Ruiz, M. Vallet-Regí, Y.K. Gun'ko, Amino-functionalized mesoporous silica nanoparticle-encapsulated octahedral organoruthenium complex as an efficient platform for combatting cancer, Inorg. Chem. 59 (2020) 10275–10284, https://doi.org/10.1021/acs.inorgchem.0c01436.
[23] W. Chen, C.A. Glackin, M.A. Horwitz, J.I. Zink, Nanomachines and other caps on mesoporous silica nanoparticles for drug delivery, Acc. Chem. Res. 52 (2019) 1531–1542.
[24] N.Ž. Knežević, I. Gadjanski, J.-O. Durand, Magnetic nanoarchitectures for cancer sensing, imaging and therapy, J. Mater. Chem. B 7 (2019) 9–23, https://doi.org/10.1039/C8TB02741B.
[25] N. Knežević, G.N. Kaluderović, Silicon-based nanotheranostics, Nanoscale. 9 (2017) 12821–12829, https://doi.org/10.1039/c7nr04445c.
[26] A. García-Fernández, E. Aznar, R. Martínez-Máñez, F. Sancenón, New advances in in vivo applications of gated mesoporous silica as drug delivery nanocarriers, Small. 16 (2020) 1902242, https://doi.org/10.1002/smll.201902242.
[27] A. Llopis-Lorente, B. Lozano-Torres, A. Bernardos, R. Martínez-Máñez, F. Sancenón, Mesoporous silica materials for controlled delivery based on enzymes, J. Mater. Chem. B 5 (2017) 3069–3083, https://doi.org/10.1039/C7TB00348J.
[28] H. Mekaru, J. Lu, F. Tamanoi, Development of mesoporous silica-based nanoparticles with controlled release capability for cancer therapy, Adv. Drug Deliv. Rev. 95 (2015) 40–49.
[29] S. Barui, V. Cauda, Multimodal decorations of mesoporous silica nanoparticles for improved cancer therapy, Pharmaceutics. 12 (2020) 1–33, https://doi.org/10.3390/pharmaceutics12060527.
[30] J.G. Croissant, K.S. Butler, J.I. Zink, C.J. Brinker, Synthetic amorphous silica nanoparticles: toxicity, biomedical and environmental implications, Nat. Rev. Mater. 5 (2020) 886–909, https://doi.org/10.1038/s41578-020-0230-0.
[31] Y. Alyassin, E.G. Sayed, P. Mehta, K. Ruparelia, M.S. Arshad, M. Rasekh, J. Shepherd, I. Kucuk, P.B. Wilson, N. Singh, M.W. Chang, D.G. Fatouros, Z. Ahmad, Application of mesoporous silica nanoparticles as drug delivery carriers for chemotherapeutic agents, Drug Discov. Today 25 (2020) 1513–1520, https://doi.org/10.1016/j.drudis.2020.06.006.
[32] J.G. Croissant, Y. Fatieiev, A. Almalik, N.M. Khashab, Mesoporous silica and organosilica nanoparticles: physical chemistry, biosafety, delivery strategies, and biomedical applications, Adv. Healthc. Mater. 7 (2018), https://doi.org/10.1002/adhm.201700831.
[33] M. Manzano, M. Vallet-Regí, Mesoporous silica nanoparticles for drug delivery, Adv. Funct. Mater. 30 (2020) 1902634, https://doi.org/10.1002/adfm.201902634.
[34] C. Chen, T. Ma, W. Tang, X. Wang, Y. Wang, J. Zhuang, Y. Zhu, P. Wang, Reversibly-regulated drug release using poly (tannic acid) fabricated nanocarriers for reduced secondary side effects in tumor therapy, Nanoscale Horizons. 5 (2020) 986–998.
[35] Y. Li, Y. Miao, M. Chen, X. Chen, F. Li, X. Zhang, Y. Gan, Stepwise targeting and responsive lipid-coated nanoparticles for enhanced tumor cell sensitivity and hepatocellular carcinoma therapy, Theranostics. 10 (2020) 3722–3736, https://doi.org/10.7150/thno.42008.
[36] W. Chen, G. Luo, Q. Lei, F. Cao, J. Fan, W. Qiu, Biomaterials rational design of multifunctional magnetic mesoporous silica nanoparticle for tumor-targeted magnetic resonance imaging and precise therapy, Biomaterials. 76 (2016) 87–101, https://doi.org/10.1016/j.biomaterials.2015.10.053.
[37] Y. Zhang, Z. Hou, Y. Ge, K. Deng, B. Liu, X. Li, Q. Li, Z. Cheng, P. Ma, C. Li, J. Lin, DNA-hybrid-gated photothermal mesoporous silica nanoparticles for NIR-responsive and aptamer-targeted drug delivery, ACS Appl. Mater. Interfaces 7 (2015) 20696–20706, https://doi.org/10.1021/acsami.5b05522.
[38] J.G. Croissant, C. Qi, O. Mongin, V. Hugues, M. Blanchard-Desce, L. Raehm, X. Cattoën, M.W.C. Man, M. Maynadier, M. Gary-Bobo, Disulfide-gated mesoporous silica nanoparticles designed for two-photon-triggered drug release and imaging, J. Mater. Chem. B 3 (2015) 6456–6461.
[39] Z. Xu, H. Liu, H. Tian, F. Yan, Real-time imaging tracking of engineered macrophages as ultrasound-triggered cell bombs for cancer treatment, Adv. Funct. Mater. 30 (2020) 1910304.
[40] J. Lai, B.P. Shah, Y. Zhang, L. Yang, K.-B. Lee, Real-time monitoring of ATP-responsive drug release using mesoporous-silica-coated multicolor upconversion nanoparticles, ACS Nano 9 (2015) 5234–5245.
[41] H. Lu, Q. Zhao, X. Wang, Y. Mao, C. Chen, Y. Gao, C. Sun, S. Wang, Multi-stimuli responsive mesoporous silica-coated carbon nanoparticles for chemo-photothermal therapy of tumor, Colloids Surf. B: Biointerfaces 190 (2020), 110941, https://doi.org/10.1016/j.colsurfb.2020.110941.
[42] L. Wan, Z. Chen, Y. Deng, T. Liao, Y. Kuang, J. Liu, J. Duan, Z. Xu, B. Jiang, C. Li, A novel intratumoral pH/redox-dual-responsive nanoplatform for cancer MR imaging and therapy, J. Colloid Interface Sci. 573 (2020) 263–277, https://doi.org/10.1016/j.jcis.2020.04.026.
[43] E. Li, Y. Yang, G. Hao, X. Yi, S. Zhang, Y. Pan, B. Xing, Multifunctional Magnetic Mesoporous Silica Nanoagents for in vivo Enzyme-Responsive Drug Delivery and MR Imaging, Nanotheranostics 2 (2018) 233–242, https://doi.org/10.7150/ntno.25565.
[44] C. Wang, N. Zhao, Y. Huang, R. He, S. Xu, W. Yuan, Coordination of injectable self-healing hydrogel with Mn-Zn ferrite@mesoporous silica nanospheres for tumor MR imaging and efficient synergistic magnetothermal-chemo-chemodynamic therapy, Chem. Eng. J. 401 (2020) 126100, https://doi.org/10.1016/j.cej.2020.126100.
[45] K. He, J. Li, Y. Shen, Y. Yu, PH-Responsive polyelectrolyte coated gadolinium oxide-doped mesoporous silica nanoparticles (Gd2O3@MSNs) for synergistic drug delivery and magnetic resonance imaging enhancement, J. Mater. Chem. B 7 (2019) 6840–6854, https://doi.org/10.1039/c9tb01654f.
[46] W. Fang, W. Zhu, H. Chen, H. Zhang, S. Hong, W. Wei, T. Zhao, MRI enhancement and tumor targeted drug delivery using Zn2+-doped Fe3O4 core/mesoporous silica shell nanocomposites, ACS Appl. Bio Mater. 3 (2020) 1690–1697, https://doi.org/10.1021/acsabm.9b01244.
[47] C. Xu, J. Nam, H. Hong, Y. Xu, J.J. Moon, Positron emission tomography-guided photodynamic therapy with biodegradable mesoporous silica nanoparticles for personalized cancer immunotherapy, ACS Nano 13 (2019) 12148–12161, https://doi.org/10.1021/acsnano.9b06691.
[48] J. Yin, Y. Zhang, D. Ma, R. Yang, F. Xu, H. Wu, C. He, L. Liu, J. Dong, Y. Shao, Nanoassembly and Multiscale Computation of Multifunctional Optical-Magnetic Nanoprobes for Tumor-Targeted Theranostics, ACS Appl. Mater. Interfaces 11 (2019) 41069–41081, https://doi.org/10.1021/acsami.9b14668.
[49] W.H. Chen, G.F. Luo, W.X. Qiu, Q. Lei, L.H. Liu, S.B. Wang, X.Z. Zhang, Mesoporous silica-based versatile theranostic nanoplatform constructed by layer-by-layer assembly for excellent photodynamic/chemo therapy, Biomaterials. 117 (2017) 54–65, https://doi.org/10.1016/j.biomaterials.2016.11.057.
[50] H. Yang, Y. Chen, Z. Chen, Y. Geng, X. Xie, X. Shen, T. Li, S. Li, C. Wu, Y. Liu, Chemo-photodynamic combined gene therapy and dual-modal cancer imaging achieved by pH-responsive alginate/chitosan multilayer-modified magnetic mesoporous silica nanocomposites, Biomater. Sci. 5 (2017) 1001–1013, https://doi.org/10.1039/C7BM00043J.
[51] X. Li, L. Xing, K. Zheng, P. Wei, L. Du, M. Shen, X. Shi, Formation of gold nanostar-coated hollow mesoporous silica for tumor multimodality imaging and photothermal therapy, ACS Appl. Mater. Interfaces 9 (2017) 5817–5827, https://doi.org/10.1021/acsami.6b15185.
[52] Q. Sun, Q. You, J. Wang, L. Liu, Y. Wang, Y. Song, Y. Cheng, S. Wang, F. Tan, N. Li, Theranostic nanoplatform: triple-modal imaging-guided synergistic cancer therapy based on liposome-conjugated mesoporous silica nanoparticles, ACS Appl. Mater. Interfaces 10 (2018) 1963–1975.
[53] C. Huang, Z. Zhang, Q. Guo, L. Zhang, F. Fan, Y. Qin, H. Wang, S. Zhou, W. Ou-Yang, H. Sun, X. Leng, X. Pan, D. Kong, L. Zhang, D. Zhu, A dual-model imaging theragnostic system based on mesoporous silica nanoparticles for enhanced cancer phototherapy, Adv. Healthc. Mater. 8 (2019) 1–14, https://doi.org/10.1002/adhm.201900840.
[54] H. Gao, X. Liu, W. Tang, D. Niu, B. Zhou, H. Zhang, W. Liu, B. Gu, X. Zhou, Y. Zheng, Y. Sun, X. Jia, L. Zhou, 99mTc-conjugated manganese-based mesoporous silica nanoparticles for SPECT, pH-responsive MRI and anti-cancer drug delivery, Nanoscale. 8 (2016) 19573–19580, https://doi.org/10.1039/c6nr07062k.
[55] S. Shi, F. Chen, S. Goel, S.A. Graves, H. Luo, C.P. Theuer, J.W. Engle, W. Cai, In vivo tumor-targeted dual-modality PET/optical imaging with a yolk/shell-structured silica nanosystem, Nano-Micro Lett. 10 (2018), 65, https://doi.org/10.1007/s40820-018-0216-2.
[56] W. Tian, Y. Su, Y. Tian, S. Wang, X. Su, Y. Liu, Y. Zhang, Y. Tang, Q. Ni, W. Liu, M. Dang, C. Wang, J. Zhang, Z. Teng, G. Lu, Periodic mesoporous organosilica coated prussian blue for MR/PA dual-modal imaging-guided photothermal-chemotherapy of triple negative breast cancer, Adv. Sci. 4 (2017) 1–10, https://doi.org/10.1002/advs.201600356.
[57] S. Fang, J. Lin, C. Li, P. Huang, W. Hou, C. Zhang, J. Liu, S. Huang, Y. Luo, W. Fan, D. Cui, Y. Xu, Z. Li, Dual-stimuli responsive nanotheranostics for multimodal imaging guided trimodal synergistic therapy, Small. 13 (2017) 1–9, https://doi.org/10.1002/smll.201602580.
[58] A. Samykutty, W.E. Grizzle, B.L. Fouts, M.W. McNally, P. Chuong, A. Thomas, A. Chiba, D. Otali, A. Woloszynska, N. Said, P.J. Frederick, J. Jasinski, J. Liu, L. R. McNally, Optoacoustic imaging identifies ovarian cancer using a microenvironment targeted theranostic wormhole mesoporous silica

nanoparticle, Biomaterials. 182 (2018) 114–126, https://doi.org/10.1016/j.biomaterials.2018.08.001.
[59] L. Shao, Y. Li, F. Huang, X. Wang, J. Lu, F. Jia, Z. Pan, X. Cui, G. Ge, X. Deng, Y. Wu, Complementary autophagy inhibition and glucose metabolism with rattle-structured polydopamine@mesoporous silica nanoparticles for augmented low-temperature photothermal therapy and in vivo photoacoustic imaging, Theranostics. 10 (2020) 7273–7286, https://doi.org/10.7150/thno.44668.
[60] Y.J. Ho, C.H. Wu, Q. Feng Jin, C.Y. Lin, P.H. Chiang, N. Wu, C.H. Fan, C.M. Yang, C.K. Yeh, Superhydrophobic drug-loaded mesoporous silica nanoparticles capped with β-cyclodextrin for ultrasound image-guided combined antivascular and chemo-sonodynamic therapy, Biomaterials 232 (2020), https://doi.org/10.1016/j.biomaterials.2019.119723.
[61] L. Pascual, C. Cerqueira-Coutinho, A. García-Fernández, B. de Luis, E. S. Bernardes, M.S. Albernaz, S. Missailidis, R. Martínez-Máñez, R. Santos-Oliveira, M. Orzaez, F. Sancenón, MUC1 aptamer-capped mesoporous silica nanoparticles for controlled drug delivery and radio-imaging applications, Nanomed. Nanotechnol. Biol. Med. 13 (2017) 2495–2505, https://doi.org/10.1016/j.nano.2017.08.006.
[62] J. Lee, J. Kim, D.G. You, S. Kim, W. Um, J. Jeon, C.H. Kim, H. Joo, G. Yi, J. H. Park, Cavitation-inducible mesoporous silica–titania nanoparticles for cancer sonotheranostics, Adv. Healthc. Mater. 9 (2020) 2000877.
[63] B. Ding, S. Shao, H. Xiao, C. Sun, X. Cai, F. Jiang, X. Zhao, P. Ma, J. Lin, MnFe2O4-decorated large-pore mesoporous silica-coated upconversion nanoparticles for near-infrared light-induced and O2 self-sufficient photodynamic therapy, Nanoscale. 11 (2019) 14654–14667, https://doi.org/10.1039/C9NR04858H.
[64] W. Sun, T. Shi, L. Luo, X. Chen, P. Lv, Y. Lv, Y. Zhuang, J. Zhu, G. Liu, X. Chen, H. Chen, Monodisperse and uniform mesoporous silicate nanosensitizers achieve low-dose X-ray-induced deep-penetrating photodynamic therapy, Adv. Mater. 31 (2019) 1808024, https://doi.org/10.1002/adma.201808024.
[65] Z. Xie, X. Cai, C. Sun, S. Liang, S. Shao, S. Huang, Z. Cheng, M. Pang, B. Xing, A. A. Al Kheraif, J. Lin, O2-loaded pH-responsive multifunctional nanodrug carrier for overcoming hypoxia and highly efficient chemo-photodynamic cancer therapy, Chem. Mater. 31 (2019) 483–490, https://doi.org/10.1021/acs.chemmater.8b04321.
[66] J. Kim, H.R. Cho, H. Jeon, D. Kim, C. Song, N. Lee, S.H. Choi, T. Hyeon, Continuous O2-evolving MnFe2O4 nanoparticle-anchored mesoporous silica nanoparticles for efficient photodynamic therapy in hypoxic cancer, J. Am. Chem. Soc. 139 (2017) 10992–10995, https://doi.org/10.1021/jacs.7b05559.
[67] J. Liu, H. Liang, M. Li, Z. Luo, J. Zhang, X. Guo, K. Cai, Tumor acidity activating multifunctional nanoplatform for NIR-mediated multiple enhanced photodynamic and photothermal tumor therapy, Biomaterials. 157 (2018) 107–124, https://doi.org/10.1016/j.biomaterials.2017.12.003.
[68] X. Hu, C. Mandika, L. He, Y. You, Y. Chang, J. Wang, T. Chen, X. Zhu, Construction of urokinase-type plasminogen activator receptor-targeted heterostructures for efficient photothermal chemotherapy against cervical cancer to achieve simultaneous anticancer and antiangiogenesis, ACS Appl. Mater. Interfaces 11 (2019) 39688–39705, https://doi.org/10.1021/acsami.9b15751.
[69] Y. Huang, K. Shen, Y. Si, C. Shan, H. Guo, M. Chen, L. Wu, Dendritic organosilica nanospheres with large mesopores as multi-guests vehicle for photoacoustic/ultrasound imaging-guided photodynamic therapy, J. Colloid Interface Sci. 583 (2021) 166–177, https://doi.org/10.1016/j.jcis.2020.09.028.
[70] X. Wang, Y. Tian, X. Liao, Y. Tang, Q. Ni, J. Sun, Y. Zhao, J. Zhang, Z. Teng, G. Lu, Enhancing selective photosensitizer accumulation and oxygen supply for high-efficacy photodynamic therapy toward glioma by 5-aminolevulinic acid loaded nanoplatform, J. Colloid Interface Sci. 565 (2020) 483–493, https://doi.org/10.1016/j.jcis.2020.01.020.
[71] R. Lv, X. Jiang, F. Yang, Y. Wang, M. Feng, J. Liu, J. Tian, Degradable magnetic-response photoacoustic/up-conversion luminescence imaging-guided photodynamic/photothermal antitumor therapy, Biomater. Sci. 7 (2019) 4558–4567, https://doi.org/10.1039/c9bm00853e.
[72] S. Yang, Q. You, L. Yang, P. Li, Q. Lu, S. Wang, F. Tan, Y. Ji, N. Li, Rodlike MSN@Au nanohybrid-modified supermolecular photosensitizer for NIRF/MSOT/CT/MR quadmodal imaging-guided photothermal/photodynamic cancer therapy, ACS Appl. Mater. Interfaces 11 (2019) 6777–6788, https://doi.org/10.1021/acsami.8b19565.
[73] S. Goel, C.A. Ferreira, F. Chen, P.A. Ellison, C.M. Siamof, T.E. Barnhart, W. Cai, Activatable hybrid nanotheranostics for tetramodal imaging and synergistic photothermal/photodynamic therapy, Adv. Mater. 30 (2018) 1–9, https://doi.org/10.1002/adma.201704367.
[74] P. Huang, X. Qian, Y. Chen, L. Yu, H. Lin, L. Wang, Y. Zhu, J. Shi, Metalloporphyrin-encapsulated biodegradable nanosystems for highly efficient magnetic resonance imaging-guided sonodynamic cancer therapy, J. Am. Chem. Soc. 139 (2017) 1275–1284, https://doi.org/10.1021/jacs.6b11846.
[75] P. Kalluru, R. Vankayala, C.S. Chiang, K.C. Hwang, Unprecedented "All-in-One" Lanthanide-doped mesoporous silica frameworks for fluorescence/MR imaging and combination of NIR light triggered chemo-photodynamic therapy of tumors, Adv. Funct. Mater. 26 (2016) 7908–7920, https://doi.org/10.1002/adfm.201603749.
[76] L. Chen, X. Zhou, W. Nie, Q. Zhang, W. Wang, Y. Zhang, C. He, Multifunctional redox-responsive mesoporous silica nanoparticles for efficient targeting drug delivery and magnetic resonance imaging, ACS Appl. Mater. Interfaces 8 (2016) 33829–33841, https://doi.org/10.1021/acsami.6b11802.
[77] F. Chen, H. Hong, S. Goel, S.A. Graves, H. Orbay, E.B. Ehlerding, S. Shi, C. P. Theuer, R.J. Nickles, W. Cai, In vivo tumor vasculature targeting of CuS@MSN based theranostic nanomedicine, ACS Nano 9 (2015) 3926–3934, https://doi.org/10.1021/nn507241v.
[78] A. Baeza, M. Colilla, M. Vallet-Regí, Advances in mesoporous silica nanoparticles for targeted stimuli-responsive drug delivery, Expert Opin. Drug Deliv. 12 (2015) 319–337, https://doi.org/10.1517/17425247.2014.953051.
[79] Y. Yang, C. Yu, Advances in silica based nanoparticles for targeted cancer therapy, Nanomed. Nanotechnol. Biol. Med. 12 (2016) 317–332, https://doi.org/10.1016/j.nano.2015.10.018.
[80] F. Dilnawaz, Multifunctional mesoporous silica nanoparticles for cancer therapy and imaging, Curr. Med. Chem. 26 (2019) 5745–5763, https://doi.org/10.2174/0929867325666180501101044.
[81] N.Ž. Knežević, J.-O. Durand, Targeted treatment of cancer with nanotherapeutics based on mesoporous silica nanoparticles, Chempluschem. 80 (2015) 26–36, https://doi.org/10.1002/cplu.201402369.
[82] K. Greish, Enhanced permeability and retention of macromolecular drugs in solid tumors: A royal gate for targeted anticancer nanomedicines, J. Drug Target. 15 (2007) 457–464, https://doi.org/10.1080/10611860701539584.
[83] M. Mladenović, I. Morgan, N. Ilić, M. Saoud, M.V. Pergal, G.N. Kaluđerović, N.Ž. Knežević, pH-responsive release of ruthenium metallotherapeutics from mesoporous silica-based nanocarriers, Pharmaceutics 13 (2021), 460, https://doi.org/10.3390/pharmaceutics13040460.
[84] F. Li, Y. Qin, J. Lee, H. Liao, N. Wang, T.P. Davis, R. Qiao, D. Ling, Stimuli-responsive nano-assemblies for remotely controlled drug delivery, J. Control. Release 322 (2020) 566–592, https://doi.org/10.1016/j.jconrel.2020.03.051.
[85] D.F. Costa, L.P. Mendes, V.P. Torchilin, The effect of low- and high-penetration light on localized cancer therapy, Adv. Drug Deliv. Rev. 138 (2019) 105–116, https://doi.org/10.1016/j.addr.2018.09.004.
[86] M. van Elk, B.P. Murphy, T. Eufrásio-da-Silva, D.P. O'Reilly, T. Vermonden, W. E. Hennink, G.P. Duffy, E. Ruiz-Hernández, Nanomedicines for advanced cancer treatments: Transitioning towards responsive systems, Int. J. Pharm. 515 (2016) 132–164, https://doi.org/10.1016/j.ijpharm.2016.10.013.
[87] E. Ruiz-Hernández, A. Baeza, M. Vallet-Regí, Smart drug delivery through DNA/magnetic nanoparticle gates, ACS Nano 5 (2011) 1259–1266, https://doi.org/10.1021/nn1029229.
[88] Y. Matsumura, H. Maeda, A new concept for macromolecular therapeutics in cancer chemotherapy: mechanism of tumoritropic accumulation of proteins and the antitumor agent smancs, Cancer Res. 46 (1986) 6387–6392.
[89] K. Stockhofe, J.M. Postema, H. Schieferstein, T.L. Ross, Radiolabeling of nanoparticles and polymers for PET imaging, Pharm. 7 (2014), https://doi.org/10.3390/ph7040392.
[90] A. Watermann, J. Brieger, Mesoporous silica nanoparticles as drug delivery vehicles in cancer, Nanomaterials 7 (2017), https://doi.org/10.3390/nano7070189.
[91] X. Huang, L. Li, T. Liu, N. Hao, H. Liu, D. Chen, F. Tang, The shape effect of mesoporous silica nanoparticles on biodistribution, clearance, and biocompatibility in vivo, ACS Nano 5 (2011) 5390–5399, https://doi.org/10.1021/nn200365a.
[92] L. Li, T. Liu, C. Fu, L. Tan, X. Meng, H. Liu, Biodistribution, excretion, and toxicity of mesoporous silica nanoparticles after oral administration depend on their shape, Nanomedicine. 11 (2015) 1915–1924, https://doi.org/10.1016/j.nano.2015.07.004.
[93] D. Shao, M.-M. Lu, Y.-W. Zhao, F. Zhang, Y.-F. Tan, X. Zheng, Y. Pan, X.-A. Xiao, Z. Wang, W.-F. Dong, J. Li, L. Chen, The shape effect of magnetic mesoporous silica nanoparticles on endocytosis, biocompatibility and biodistribution, Acta Biomater. 49 (2017) 531–540, https://doi.org/10.1016/j.actbio.2016.11.007.
[94] M.F. Attia, N. Anton, J. Wallyn, Z. Omran, T.F. Vandamme, An overview of active and passive targeting strategies to improve the nanocarriers efficiency to tumour sites, J. Pharm. Pharmacol. 71 (2019) 1185–1198, https://doi.org/10.1111/jphp.13098.
[95] I.I. Slowing, C.-W. Wu, J.L. Vivero-Escoto, V.S.-Y. Lin, Mesoporous silica nanoparticles for reducing hemolytic activity towards mammalian red blood cells, Small. 5 (2009) 57–62, https://doi.org/10.1002/smll.200800926.
[96] Y. Chen, P. Xu, H. Chen, Y. Li, W. Bu, Z. Shu, Y. Li, J. Zhang, L. Zhang, L. Pan, X. Cui, Z. Hua, J. Wang, L. Zhang, J. Shi, Colloidal HPMO nanoparticles: Silica-etching chemistry tailoring, topological transformation, and nano-biomedical applications, Adv. Mater. 25 (2013) 3100–3105, https://doi.org/10.1002/adma.201204685.
[97] Z. Teng, S. Wang, X. Su, G. Chen, Y. Liu, Z. Luo, W. Luo, Y. Tang, H. Ju, D. Zhao, G. Lu, Facile synthesis of yolk-shell structured inorganic-organic hybrid spheres with ordered radial mesochannels, Adv. Mater. 26 (2014) 3741–3747, https://doi.org/10.1002/adma.201400136.
[98] Q. He, J. Zhang, J. Shi, Z. Zhu, L. Zhang, W. Bu, L. Guo, Y. Chen, The effect of PEGylation of mesoporous silica nanoparticles on nonspecific binding of serum proteins and cellular responses, Biomaterials. 31 (2010) 1085–1092, https://doi.org/10.1016/j.biomaterials.2009.10.046.
[99] F. Tang, L. Li, D. Chen, Mesoporous silica nanoparticles: Synthesis, biocompatibility and drug delivery, Adv. Mater. 24 (2012) 1504–1534, https://doi.org/10.1002/adma.201104763.
[100] S. Sean, et al., Biocompatibility of multi-imaging engineered mesoporous silica nanoparticles: in vitro and adult and fetal in vivo studies, J. Biomed. Nanotechnol. 13 (2017) 544–558, https://doi.org/10.1166/jbn.2017.2369.Biocompatibility.
[101] J. Lu, M. Liong, Z. Li, J.I. Zink, F. Tamanoi, Biocompatibility, biodistribution, and drug-delivery efficiency of mesoporous silica nanoparticles for cancer therapy in animals, Small. 6 (2010) 1794–1805, https://doi.org/10.1002/smll.201000538.

[102] W. Lei, C. Sun, T. Jiang, Y. Gao, Y. Yang, Q. Zhao, S. Wang, Polydopamine-coated mesoporous silica nanoparticles for multi-responsive drug delivery and combined chemo-photothermal therapy, Mater. Sci. Eng. C 105 (2019) 110103, https://doi.org/10.1016/j.msec.2019.110103.
[103] N. Poonia, V. Lather, D. Pandita, Mesoporous silica nanoparticles: a smart nanosystem for management of breast cancer, Drug Discov. Today 23 (2018) 315–332, https://doi.org/10.1016/j.drudis.2017.10.022.
[104] J. Mo, L. He, B. Ma, T. Chen, Tailoring particle size of mesoporous silica nanosystem to antagonize glioblastoma and overcome blood-brain barrier, ACS Appl. Mater. Interfaces 8 (2016) 6811–6825, https://doi.org/10.1021/acsami.5b11730.
[105] F. Zhao, C. Zhang, C. Zhao, W. Gao, X. Fan, G. Wu, A facile strategy to fabricate a pH-responsive mesoporous silica nanoparticle end-capped with amphiphilic peptides by self-assembly, Colloids Surf. B: Biointerfaces 179 (2019) 352–362, https://doi.org/10.1016/j.colsurfb.2019.03.019.
[106] J.S. Desgrosellier, D.A. Cheresh, Integrins in cancer: Biological implications and therapeutic opportunities, Nat. Rev. Cancer 10 (2010) 9–22, https://doi.org/10.1038/nrc2748.
[107] J. Hu, X. Zhang, Z. Wen, Y. Tan, N. Huang, S. Cheng, H. Zheng, Y. Cheng, Asn-Gly-Arg-modified polydopamine-coated nanoparticles for dual-targeting therapy of brain glioma in rats, Oncotarget 7 (2016) 73681–73696, https://doi.org/10.18632/oncotarget.12047.
[108] L. Guzman-Rojas, R. Rangel, A. Salameh, J.K. Edwards, E. Dondossola, Y.G. Kim, A. Saghatelian, R.J. Giordano, M.G. Kolonin, F.I. Staquicini, E. Koivunen, R. L. Sidman, W. Arap, R. Pasqualini, Cooperative effects of aminopeptidase N (CD13) expressed by nonmalignant and cancer cells within the tumor microenvironment, Proc. Natl. Acad. Sci. U. S. A. 109 (2012) 1637–1642, https://doi.org/10.1073/pnas.1120790109.
[109] M.M. Khan, N. Filipczak, V.P. Torchilin, Cell penetrating peptides: A versatile vector for co-delivery of drug and genes in cancer, J. Control. Release 330 (2021) 1220–1228, https://doi.org/10.1016/j.jconrel.2020.11.028.
[110] I. Gessner, I. Neundorf, Nanoparticles modified with cell-penetrating peptides: Conjugation mechanisms, physicochemical properties, and application in cancer diagnosis and therapy, Int. J. Mol. Sci. 21 (2020) 1–21, https://doi.org/10.3390/ijms21072536.
[111] X. Chen, H. Sun, J. Hu, X. Han, H. Liu, Y. Hu, Transferrin gated mesoporous silica nanoparticles for redox-responsive and targeted drug delivery, Colloids Surf. B: Biointerfaces 152 (2017) 77–84, https://doi.org/10.1016/j.colsurfb.2017.01.010.
[112] Y. Shen, X. Li, D. Dong, B. Zhang, Y. Xue, P. Shang, Transferrin receptor 1 in cancer: a new sight for cancer therapy, Am. J. Cancer Res. 8 (2018) 916–931.
[113] S. Sigismund, D. Avanzato, L. Lanzetti, Emerging Functions of the EGFR in Cancer, Mol. Oncol. 12 (2018) 3–20, https://doi.org/10.1002/1878-0261.12155.
[114] H.L. Goel, A.M. Mercurio, VEGF targets the tumour cell, Nat. Rev. Cancer 13 (2013) 871–882, https://doi.org/10.1038/nrc3627.
[115] H. Attarwala, Role of antibodies in cancer targeting, J. Nat. Sci. Biol. Med. 1 (2010) 53–56, https://doi.org/10.4103/0976-9668.71675.
[116] M. Ovacik, K. Lin, Tutorial on monoclonal antibody pharmacokinetics and its considerations in early development, Clin. Transl. Sci. 11 (2018) 540–552, https://doi.org/10.1111/cts.12567.
[117] D. Dréau, L.J. Moore, M.P. Alvarez-Berrios, M. Tarannum, P. Mukherjee, J. L. Vivero-Escoto, Mucin-1-antibody-conjugated mesoporous silica nanoparticles for selective breast cancer detection in a mucin-1 transgenic murine mouse model, J. Biomed. Nanotechnol. 12 (2016) 2172–2184, https://doi.org/10.1166/jbn.2016.2318.
[118] S. Goel, F. Chen, S. Luan, H.F. Valdovinos, S. Shi, S.A. Graves, F. Ai, T.E. Barnhart, C.P. Theuer, W. Cai, Engineering intrinsically zirconium-89 radiolabeled self-destructing mesoporous silica nanostructures for in vivo biodistribution and tumor targeting studies, Adv. Sci. 3 (2016) 1–11, https://doi.org/10.1002/advs.201600122.
[119] C. Lin, B.C.K. Wong, H. Chen, Z. Bian, G. Zhang, X. Zhang, M. Kashif Riaz, D. Tyagi, G. Lin, Y. Zhang, J. Wang, A. Lu, Z. Yang, Pulmonary delivery of triptolide-loaded liposomes decorated with anti-carbonic anhydrase IX antibody for lung cancer therapy, Sci. Rep. 7 (2017) 1–12, https://doi.org/10.1038/s41598-017-00957-4.
[120] M.Y. Mboge, B.P. Mahon, R. McKenna, S.C. Frost, Carbonic anhydrases: Role in pH control and cancer, Metabolites 8 (2018), 19, https://doi.org/10.3390/metabo8010019.
[121] Z. Fu, J. Xiang, Aptamers, the nucleic acid antibodies, in cancer therapy, Int. J. Mol. Sci. 21 (2020), 2793, https://doi.org/10.3390/ijms21082793.
[122] J. Zhou, J. Rossi, Aptamers as targeted therapeutics: current potential and challenges, Nat. Rev. Drug Discov. 16 (2017) 181–202, https://doi.org/10.1038/nrd.2016.199.
[123] Y. Li, Y. Duo, J. Bi, X. Zeng, L. Mei, S. Bao, L. He, A. Shan, Y. Zhang, X. Yu, Targeted delivery of anti-miR-155 by functionalized mesoporous silica nanoparticles for colorectal cancer therapy, Int. J. Nanomedicine 13 (2018) 1241–1256, https://doi.org/10.2147/IJN.S158290.
[124] Y. Morita, M. Leslie, H. Kameyama, D.E. Volk, T. Tanaka, Aptamer therapeutics in cancer: current and future, Cancers (Basel). 10 (2018), 80, https://doi.org/10.3390/cancers10030080.
[125] Y. Tang, H. Hu, M.G. Zhang, J. Song, L. Nie, S. Wang, G. Niu, P. Huang, G. Lu, X. Chen, An aptamer-targeting photoresponsive drug delivery system using "off-on" graphene oxide wrapped mesoporous silica nanoparticles, Nanoscale. 7 (2015) 6304–6310, https://doi.org/10.1039/c4nr07493a.
[126] M.Y. Hanafi-Bojd, S.A. Moosavian Kalat, S.M. Taghdisi, L. Ansari, K. Abnous, B. Malaekeh-Nikouei, MUC1 aptamer-conjugated mesoporous silica nanoparticles effectively target breast cancer cells, Drug Dev. Ind. Pharm. 44 (2018) 13–18, https://doi.org/10.1080/03639045.2017.1371734.
[127] N. Iqbal, N. Iqbal, Human epidermal growth factor receptor 2 (HER2) in cancers: overexpression and therapeutic implications, Mol. Biol. Int. 2014 (2014) 1–9, https://doi.org/10.1155/2014/852748.
[128] J. Zhang, Y. Shen, M. Li, T. Liu, J. Liu, Y. Xie, S. Xu, H. Liu, A dual-functional her2 aptamer-conjugated, ph-activated mesoporous silica nanocarrier-based drug delivery system provides in vitro synergistic cytotoxicity in her2-positive breast cancer cells, Int. J. Nanomedicine 14 (2019) 4029–4044, https://doi.org/10.2147/IJN.S201688.
[129] L. Huang, J. Liu, F. Gao, Q. Cheng, B. Lu, H. Zheng, H. Xu, P. Xu, X. Zhang, X. Zeng, A dual-responsive, hyaluronic acid targeted drug delivery system based on hollow mesoporous silica nanoparticles for cancer therapy, J. Mater. Chem. B 6 (2018) 4618–4629, https://doi.org/10.1039/c8tb00989a.
[130] S.A. Shahin, R. Wang, S.I. Simargi, A. Contreras, L. Parra Echavarria, L. Qu, W. Wen, T. Dellinger, J. Unternaehrer, F. Tamanoi, J.I. Zink, C.A. Glackin, Hyaluronic acid conjugated nanoparticle delivery of siRNA against TWIST reduces tumor burden and enhances sensitivity to cisplatin in ovarian cancer, Nanomed. Nanotechnol. Biol. Med. 14 (2018) 1381–1394, https://doi.org/10.1016/j.nano.2018.04.008.
[131] V. Ricci, D. Zonari, S. Cannito, A. Marengo, M.T. Scupoli, M. Malatesta, F. Carton, F. Boschi, G. Berlier, S. Arpicco, Hyaluronated mesoporous silica nanoparticles for active targeting: influence of conjugation method and hyaluronic acid molecular weight on the nanovector properties, J. Colloid Interface Sci. 516 (2018) 484–497, https://doi.org/10.1016/j.jcis.2018.01.072.
[132] F. Du, W. Wang, Hyaluronic Acid-Modified Mesoporous Silica-Coated Superparamagnetic Fe3O4 Nanoparticles for Targeted Drug Delivery 14 (2019) 5785–5797, https://doi.org/10.2147/IJN.S213974.
[133] Y. Zhang, J. Xu, Mesoporous silica nanoparticle-based intelligent drug delivery system for bienzyme-responsive tumour targeting and controlled release, R. Soc. Open Sci. 5 (2018), https://doi.org/10.1098/rsos.170986.
[134] S.K. Jones, A. Sarkar, D.P. Feldmann, P. Hoffmann, O.M. Merkel, Revisiting the value of competition assays in folate receptor-mediated drug delivery, Biomaterials. 138 (2017) 35–45, https://doi.org/10.1016/j.biomaterials.2017.05.034.
[135] N.Ž. Knežević, J. Mrđanović, I. Borišev, S. Milenković, Đ. Janaćković, F. Cunin, A. Djordjevic, Hydroxylated fullerene-capped, vinblastine-loaded folic acid-functionalized mesoporous silica nanoparticles for targeted anticancer therapy, RSC Adv. 6 (2016) 7061–7065, https://doi.org/10.1039/C5RA22937E.
[136] P. Khosravian, M.S. Ardestani, M. Khoobi, S.N. Ostad, F.A. Dorkoosh, H.A. Javar, M. Amanlou, Mesoporous silica nanoparticles functionalized with folic acid/methionine for active targeted delivery of docetaxel, Oncol. Targets. Ther. 9 (2016) 7315–7330, https://doi.org/10.2147/OTT.S113815.
[137] Z. Li, Y. Zhang, K. Zhang, Z. Wu, N. Feng, Biotinylated-lipid bilayer coated mesoporous silica nanoparticles for improving the bioavailability and anti-leukaemia activity of Tanshinone IIA, Artif. Cells Nanomed. Biotechnol. 46 (2018) 578–587, https://doi.org/10.1080/21691401.2018.1431651.
[138] N. Thepphankulngarm, P. Wonganan, C. Sapcharoenkun, T. Tuntulani, P. Leeladee, Combining Vitamin B12 and cisplatin-loaded porous silica nanoparticles via coordination: A facile approach to prepare a targeted drug delivery system, New J. Chem. 41 (2017) 13823–13829, https://doi.org/10.1039/c7nj02754k.
[139] G. Lv, K. Li, L. Qiu, et al., Enhanced Tumor Diagnostic and Therapeutic Effect of Mesoporous Silica Nanoparticle-Mediated Pre-targeted Strategy, Pharm Res. 35 (2018) 63, https://doi.org/10.1007/s11095-017-2338-5.
[140] J. Liu, B. Zhang, Z. Luo, X. Ding, J. Li, L. Dai, J. Zhou, X. Zhao, J. Ye, K. Cai, Enzyme responsive mesoporous silica nanoparticles for targeted tumor therapy in vitro and in vivo, Nanoscale. 7 (2015) 3614–3626, https://doi.org/10.1039/C5NR00072F.
[141] E. Dalle Vedove, G. Costabile, O.M. Merkel, Mannose and mannose-6-phosphate receptor-targeted drug delivery systems and their application in cancer therapy, Adv. Healthc. Mater. 7 (2018), e1701398, https://doi.org/10.1002/adhm.201701398.
[142] K. Movahedi, S. Schoonooghe, D. Laoui, I. Houbracken, W. Waelput, K. Breckpot, L. Bouwens, T. Lahoutte, P. De Baetselier, G. Raes, N. Devoogdt, J.A. Van Ginderachter, Nanobody-based targeting of the macrophage mannose receptor for effective in vivo imaging of tumor-associated macrophages, Cancer Res. 72 (2012) 4165–4177, https://doi.org/10.1158/0008-5472.CAN-11-2994.
[143] N.Ž. Knežević, V. Stojanovic, A. Chaix, E. Bouffard, K. El Cheikh, A. Morère, M. Maynadier, G. Lemercier, M. Garcia, M. Gary-Bobo, J.-O. Durand, F. Cunin, Ruthenium(II) multifunctionalized porous silicon nanoparticles for two-photon near-infrared light responsive imaging and photodynamic cancer therapy, J. Mater. Chem. B 4 (2016) 1337–1342, https://doi.org/10.1039/C5TB02726H.
[144] A. Chaix, K. El Cheikh, E. Bouffard, M. Maynadier, D. Aggad, V. Stojanovic, N. Knezevic, M. Garcia, P. Maillard, A. Morère, M. Gary-Bobo, L. Raehm, S. Richeter, J.-O. Durand, F. Cunin, Mesoporous silicon nanoparticles for targeted two-photon theranostics of prostate cancer, J. Mater. Chem. B 4 (2016), https://doi.org/10.1039/c6tb00690f.
[145] V. Mamaeva, R. Niemi, M. Beck, E. Özliseli, D. Desai, S. Landor, T. Gronroos, P. Kronqvist, I.K.N. Pettersen, E. McCormack, J.M. Rosenholm, M. Linden, C. Sahlgren, Inhibiting notch activity in breast cancer stem cells by glucose functionalized nanoparticles carrying γ-secretase inhibitors, Mol. Ther. 24 (2016) 926–936, https://doi.org/10.1038/mt.2016.42.
[146] L. Feng, Z. Dong, D. Tao, Y. Zhang, Z. Liu, The acidic tumor microenvironment: a target for smart cancer nano-theranostics, Natl. Sci. Rev. 5 (2018) 269–286, https://doi.org/10.1093/nsr/nwx062.

[147] L.E. Gerweck, K. Seetharaman, Cellular pH gradient in tumor versus normal tissue: potential exploitation for the treatment of cancer, Cancer Res. 56 (1996) 1194–1198.
[148] Y. Kato, S. Ozawa, C. Miyamoto, Y. Maehata, A. Suzuki, T. Maeda, Y. Baba, Acidic extracellular microenvironment and cancer, Cancer Cell Int. 13 (2013) 89, https://doi.org/10.1186/1475-2867-13-89.
[149] J. Lu, B. Luo, Z. Chen, Y. Yuan, Y. Kuang, L. Wan, L. Yao, X. Chen, B. Jiang, J. Liu, Host-guest fabrication of dual-responsive hyaluronic acid/mesoporous silica nanoparticle based drug delivery system for targeted cancer therapy, Int. J. Biol. Macromol. 146 (2020) 363–373.
[150] K.-N. Yang, C.-Q. Zhang, W. Wang, P.C. Wang, J.-P. Zhou, X.-J. Liang, pH-responsive mesoporous silica nanoparticles employed in controlled drug delivery systems for cancer treatment, Cancer Biol. Med. 11 (2014) 34.
[151] X. Yuan, S. Peng, W. Lin, J. Wang, L. Zhang, Multistage pH-responsive mesoporous silica nanohybrids with charge reversal and intracellular release for efficient anticancer drug delivery, J. Colloid Interface Sci. 555 (2019) 82–93, https://doi.org/10.1016/j.jcis.2019.07.061.
[152] M. Martínez-Carmona, D. Lozano, M. Colilla, M. Vallet-Regí, Lectin-conjugated pH-responsive mesoporous silica nanoparticles for targeted bone cancer treatment, Acta Biomater. 65 (2018) 393–404, https://doi.org/10.1016/j.actbio.2017.11.007.
[153] A.-L. Lin, S.-Z. Li, C.-H. Xu, X.-S. Li, B.-Y. Zheng, J.-J. Gu, M.-R. Ke, J.-D. Huang, A pH-responsive stellate mesoporous silica based nanophotosensitizer for in vivo cancer diagnosis and targeted photodynamic therapy, Biomater. Sci. 7 (2019) 211–219.
[154] K. He, J. Li, Y. Shen, Y. Yu, PH-Responsive polyelectrolyte coated gadolinium oxide-doped mesoporous silica nanoparticles (Gd2O3@MSNs) for synergistic drug delivery and magnetic resonance imaging enhancement, J. Mater. Chem. B 7 (2019) 6840–6854, https://doi.org/10.1039/c9tb01654f.
[155] H. Yang, Y. Chen, Z. Chen, Y. Geng, X. Xie, X. Shen, T. Li, S. Li, C. Wu, Y. Liu, Biomaterials science, Biomater. Sci. 5 (2017) 1001–1013, https://doi.org/10.1039/c7bm00043j.
[156] H. Gao, X. Liu, W. Tang, D. Niu, B. Zhou, H. Zhang, W. Liu, B. Gu, X. Zhou, Y. Zheng, Y. Sun, X. Jia, L. Zhou, 99mTc-conjugated manganese-based mesoporous silica nanoparticles for SPECT, pH-responsive MRI and anti-cancer drug delivery, Nanoscale. 8 (2016) 19573–19580, https://doi.org/10.1039/c6nr07062k.
[157] F.Q. Schafer, G.R. Buettner, Redox environment of the cell as viewed through the redox state of the glutathione disulfide/glutathione couple, Free Radic. Biol. Med. 30 (2001) 1191–1212, https://doi.org/10.1016/S0891-5849(01)00480-4.
[158] D. Trachootham, J. Alexandre, P. Huang, Targeting cancer cells by ROS-mediated mechanisms: a radical therapeutic approach? Nat. Rev. Drug Discov. 8 (2009) 579–591, https://doi.org/10.1038/nrd2803.
[159] J.M. Estrela, A. Ortega, E. Obrador, Glutathione in cancer biology and therapy, Crit. Rev. Clin. Lab. Sci. 43 (2006) 143–181, https://doi.org/10.1080/10408360500523878.
[160] M.A. Wouters, S.W. Fan, N.L. Haworth, Disulfides as redox switches: from molecular mechanisms to functional significance, Antioxid. Redox Signal. 12 (2009) 53–91, https://doi.org/10.1089/ars.2009.2510.
[161] M. Chen, J. Hu, L. Wang, Y. Li, C. Zhu, C. Chen, M. Shi, Z. Ju, X. Cao, Z. Zhang, Targeted and redox-responsive drug delivery systems based on carbonic anhydrase IX-decorated mesoporous silica nanoparticles for cancer therapy, Sci. Rep. 10 (2020) 1–12, https://doi.org/10.1038/s41598-020-71071-1.
[162] M. Shahriari, M. Zahiri, K. Abnous, S.M. Taghdisi, M. Ramezani, M. Alibolandi, Enzyme responsive drug delivery systems in cancer treatment, J. Control. Release 308 (2019) 172–189, https://doi.org/10.1016/j.jconrel.2019.07.004.
[163] K.O. Paredes, D. Diana, V. Garc, L.L. Chamizo, M. Marciello, D. Miguel, S. Prashar, G. Santiago, M. Filice, Multifunctional Silica-Based Nanoparticles with Controlled Release of Organotin Metallodrug for Targeted Theranosis of Breast Cancer, Cancers (Basel) 12 (2020) 187.
[164] K. Vaghasiya, E. Ray, A. Sharma, O.P. Katare, R.K. Verma, Matrix Metalloproteinase-Responsive Mesoporous Silica Nanoparticles Cloaked with Cleavable Protein for " Self-Actuating " On-Demand Controlled Drug Delivery for Cancer Therapy, ACS Appl. Bio Mater. 3 (2020) 4987–4999, https://doi.org/10.1021/acsabm.0c00497.
[165] M. Wang, Y. Han, B. Hu, L. Teng, J. Zhou, H. Zhang, J. Chen, Enzyme-Responsive Mesoporous Silica Nanoparticles for Tumor Cells and Mitochondria Multistage-Targeted Drug Delivery, Int J Nanomedicine 14 (2019) 2533–2542, https://doi.org/10.2147/IJN.S202210.
[166] J. Zhou, M. Wang, H. Ying, D. Su, H. Zhang, G. Lu, J. Chen, Extracellular Matrix Component Shelled Nanoparticles as Dual Enzyme-Responsive Drug Delivery Vehicles for Cancer Therapy, Int J Nanomedicine 4 (2018) 2404–2411, https://doi.org/10.1021/acsbiomaterials.8b00327.
[167] W.H. Chen, G.F. Luo, W.X. Qiu, Q. Lei, L.H. Liu, S.B. Wang, X.Z. Zhang, Mesoporous silica-based versatile theranostic nanoplatform constructed by layer-by-layer assembly for excellent photodynamic/chemo therapy, Biomaterials. 117 (2017) 54–65, https://doi.org/10.1016/j.biomaterials.2016.11.057.
[168] N.Ž. Knežević, B.G. Trewyn, V.S.Y. Lin, Light- and pH-responsive release of doxorubicin from a mesoporous silica-based nanocarrier, Chem. Eur. J. 17 (2011) 3338–3342, https://doi.org/10.1002/chem.201002960.
[169] N.Z. Knežević, Visible light responsive anticancer treatment with an amsacrine-loaded mesoporous silica-based nanodevice, RSC Adv. 3 (2013) 19388–19392, https://doi.org/10.1039/c3ra43492c.
[170] M. Martínez-Carmona, D. Lozano, A. Baeza, M. Colilla, M. Vallet-Regí, A novel visible light responsive nanosystem for cancer treatment, Nanoscale 9 (2017) 15967–15973.
[171] R. Lv, X. Jiang, F. Yang, Y. Wang, M. Feng, J. Liu, J. Tian, Degradable magnetic-response photoacoustic/up-conversion luminescence imaging-guided photodynamic/photothermal antitumor therapy, Biomater. Sci. 7 (2019) 4558–4567, https://doi.org/10.1039/c9bm00853e.
[172] S. Yang, Q. You, L. Yang, P. Li, Q. Lu, S. Wang, F. Tan, Y. Ji, N. Li, Rodlike MSN@Au nanohybrid-modified supermolecular photosensitizer for NIRF/MSOT/CT/MR quadmodal imaging-guided photothermal/photodynamic cancer therapy, ACS Appl. Mater. Interfaces 11 (2019) 6777–6788, https://doi.org/10.1021/acsami.8b19565.
[173] S. Goel, C.A. Ferreira, F. Chen, P.A. Ellison, C.M. Siamof, T.E. Barnhart, W. Cai, Activatable hybrid nanotheranostics for tetramodal imaging and synergistic photothermal/photodynamic therapy, Adv. Mater. 30 (2018) 1–9, https://doi.org/10.1002/adma.201704367.
[174] Y. Huang, K. Shen, Y. Si, C. Shan, H. Guo, M. Chen, L. Wu, Dendritic organosilica nanospheres with large mesopores as multi-guests vehicle for photoacoustic/ultrasound imaging-guided photodynamic therapy, J. Colloid Interface Sci. 583 (2021) 166–177, https://doi.org/10.1016/j.jcis.2020.09.028.
[175] L. Shao, Y. Li, F. Huang, X. Wang, J. Lu, F. Jia, Z. Pan, X. Cui, G. Ge, X. Deng, Y. Wu, Complementary autophagy inhibition and glucose metabolism with rattle-structured polydopamine@mesoporous silica nanoparticles for augmented low-temperature photothermal therapy and in vivo photoacoustic imaging, Theranostics. 10 (2020) 7273–7286, https://doi.org/10.7150/thno.44668.
[176] C. Huang, Z. Zhang, Q. Guo, L. Zhang, F. Fan, Y. Qin, H. Wang, S. Zhou, W. Ou-Yang, H. Sun, X. Leng, X. Pan, D. Kong, L. Zhang, D. Zhu, A dual-model imaging theragnostic system based on mesoporous silica nanoparticles for enhanced cancer phototherapy, Adv. Healthc. Mater. 8 (2019) 1–14, https://doi.org/10.1002/adhm.201900840.
[177] E. Guisasola, L. Asín, L. Beola, J.M. de la Fuente, A. Baeza, M. Vallet-Regí, Beyond traditional hyperthermia: in vivo cancer treatment with magnetic-responsive mesoporous silica nanocarriers, ACS Appl. Mater. Interfaces 10 (2018) 12518–12525, https://doi.org/10.1021/acsami.8b02398.
[178] P. Saint-Cricq, S. Deshayes, J.I. Zink, A.M. Kasko, Magnetic field activated drug delivery using thermodegradable azo-functionalised PEG-coated core–shell mesoporous silica nanoparticles, Nanoscale. 7 (2015) 13168–13172.
[179] F. Perton, M. Tasso, G.A. Muñoz Medina, M. Ménard, C. Blanco-Andujar, E. Portiansky, M.B.F. van Raap, D. Bégin, F. Meyer, S. Begin-Colin, D. Mertz, Fluorescent and magnetic stellate mesoporous silica for bimodal imaging and magnetic hyperthermia, Appl. Mater. Today 16 (2019) 301–314, https://doi.org/10.1016/j.apmt.2019.06.006.
[180] H. Li, W. Yan, X. Suo, H. Peng, X. Yang, Z. Li, J. Zhang, D. Liu, Nucleus-targeted nano delivery system eradicates cancer stem cells by combined thermotherapy and hypoxia-activated chemotherapy, Biomaterials. 200 (2019) 1–14.
[181] C. Wang, N. Zhao, Y. Huang, R. He, S. Xu, W. Yuan, Coordination of injectable self-healing hydrogel with Mn-Zn ferrite@mesoporous silica nanospheres for tumor MR imaging and efficient synergistic magnetothermal-chemo-chemodynamic therapy, Chem. Eng. J. 401 (2020) 126100, https://doi.org/10.1016/j.cej.2020.126100.
[182] J.L. Paris, M.V. Cabañas, M. Manzano, M. Vallet-Regí, Polymer-grafted mesoporous silica nanoparticles as ultrasound-responsive drug carriers, ACS Nano 9 (2015) 11023–11033.
[183] C.-A. Cheng, W. Chen, L. Zhang, H.H. Wu, J.I. Zink, A responsive mesoporous silica nanoparticle platform for magnetic resonance imaging-guided high-intensity focused ultrasound-stimulated cargo delivery with controllable location, time, and dose, J. Am. Chem. Soc. 141 (2019) 17670–17684.
[184] Y.J. Ho, C.H. Wu, Q. Feng Jin, C.Y. Lin, P.H. Chiang, N. Wu, C.H. Fan, C.M. Yang, C.K. Yeh, Superhydrophobic drug-loaded mesoporous silica nanoparticles capped with β-cyclodextrin for ultrasound image-guided combined antivascular and chemo-sonodynamic therapy, Biomaterials 232 (2020), https://doi.org/10.1016/j.biomaterials.2019.119723.
[185] C.-A. Cheng, W. Chen, L. Zhang, H.H. Wu, J.I. Zink, Magnetic resonance imaging of high-intensity focused ultrasound-stimulated drug release from a self-reporting core@ shell nanoparticle platform, Chem. Commun. 56 (2020) 10297–10300.
[186] N.Z. Knezevic, V.S.Y. Lin, A magnetic mesoporous silica nanoparticle-based drug delivery system for photosensitive cooperative treatment of cancer with a mesopore-capping agent and mesopore-loaded drug, Nanoscale. 5 (2013) 1544–1551, https://doi.org/10.1039/c2nr33417h.
[187] Y. Gao, D. Gao, J. Shen, Q. Wang, A review of mesoporous silica nanoparticle delivery systems in chemo-based combination cancer therapies, Front. Chem. 8 (2020) 1086.
[188] M. Zhang, X. Chen, C. Li, X. Shen, Charge-reversal nanocarriers: An emerging paradigm for smart cancer nanomedicine, J. Control. Release 319 (2020) 46–62, https://doi.org/10.1016/j.jconrel.2019.12.024.
[189] W. Tian, Y. Su, Y. Tian, S. Wang, X. Su, Y. Liu, Y. Zhang, Y. Tang, Q. Ni, W. Liu, M. Dang, C. Wang, J. Zhang, Z. Teng, G. Lu, Periodic mesoporous organosilica coated prussian blue for MR/PA dual-modal imaging-guided photothermal-chemotherapy of triple negative breast cancer, Adv. Sci. 4 (2017) 1–10, https://doi.org/10.1002/advs.201600356.
[190] M. Pereira-Silva, I. Jarak, C. Alvarez-Lorenzo, A. Concheiro, A.C. Santos, F. Veiga, A. Figueiras, Micelleplexes as nucleic acid delivery systems for cancer-targeted therapies, J. Control. Release 323 (2020) 442–462, https://doi.org/10.1016/j.jconrel.2020.04.041.
[191] R. Juneja, H. Vadarevu, J. Halman, M. Tarannum, L. Rackley, J. Dobbs, J. Marquez, M. Chandler, K. Afonin, J.L. Vivero-Escoto, Combination of nucleic acid and mesoporous silica nanoparticles: optimization and therapeutic performance in vitro, ACS Appl. Mater. Interfaces 12 (2020) 38873–38886, https://doi.org/10.1021/acsami.0c07106.

[192] S. Vandghanooni, J. Barar, M. Eskandani, Y. Omidi, Aptamer-conjugated mesoporous silica nanoparticles for simultaneous imaging and therapy of cancer, TrAC Trends Anal. Chem. 123 (2020) 115759, https://doi.org/10.1016/j.trac.2019.115759.
[193] A. Noureddine, A. Maestas-Olguin, E.A. Saada, A.E. LaBauve, J.O. Agola, K. E. Baty, T. Howard, J.K. Sabo, C.R.S. Espinoza, J.A. Doudna, J.S. Schoeniger, K. S. Butler, O.A. Negrete, C.J. Brinker, R.E. Serda, Engineering of monosized lipid-coated mesoporous silica nanoparticles for CRISPR delivery, Acta Biomater. 114 (2020) 358–368, https://doi.org/10.1016/j.actbio.2020.07.027.
[194] M.I. Sajid, M. Moazzam, S. Kato, K. Yeseom Cho, R.K. Tiwari, Overcoming barriers for siRNA therapeutics: from bench to bedside, Pharmaceuticals (Basel) 13 (2020), https://doi.org/10.3390/ph13100294.
[195] M.A. Subhan, V.P. Torchilin, Efficient nanocarriers of siRNA therapeutics for cancer treatment, Transl. Res. 214 (2019) 62–91, https://doi.org/10.1016/j.trsl.2019.07.006.
[196] A.M. Carvalho, R.A. Cordeiro, H. Faneca, Silica-based gene delivery systems: from design to therapeutic applications, Pharmaceutics. 12 (2020) 649, https://doi.org/10.3390/pharmaceutics12070649.
[197] J.L. Paris, M. Vallet-Regí, Mesoporous silica nanoparticles for co-delivery of drugs and nucleic acids in oncology: a review, Pharmaceutics. 12 (2020) 526, https://doi.org/10.3390/pharmaceutics12060526.
[198] X. Xiao, Q. He, K. Huang, Novel amino-modified silica nanoparticles as efficient vector for hepatocellular carcinoma gene therapy, Med. Oncol. 27 (2010) 1200–1207, https://doi.org/10.1007/s12032-009-9359-9.
[199] Y. Tao, J. Wang, X. Xu, Emerging and innovative theranostic approaches for mesoporous silica nanoparticles in hepatocellular carcinoma: current status and advances, Front. Bioeng. Biotechnol. 8 (2020) 184, https://doi.org/10.3389/fbioe.2020.00184.
[200] J.D. Sander, J.K. Joung, CRISPR-Cas systems for editing, regulating and targeting genomes, Nat. Biotechnol. 32 (2014) 347–355, https://doi.org/10.1038/nbt.2842.
[201] A.V. Wright, J.K. Nuñez, J.A. Doudna, Biology and applications of CRISPR systems: harnessing nature's toolbox for genome engineering, Cell 164 (2016) 29–44, https://doi.org/10.1016/j.cell.2015.12.035.
[202] M. Zhang, E.A. Eshraghian, O. Al Jammal, Z. Zhang, X. Zhu, CRISPR technology: The engine that drives cancer therapy, Biomed. Pharmacother. 133 (2021) 111007, https://doi.org/10.1016/j.biopha.2020.111007.
[203] A. Mir, A. Edraki, J. Lee, E.J. Sontheimer, Type II-C CRISPR-Cas9 biology, mechanism, and application, ACS Chem. Biol. 13 (2018) 357–365, https://doi.org/10.1021/acschembio.7b00855.
[204] J.A. Doudna, E. Charpentier, Genome editing. The new frontier of genome engineering with CRISPR-Cas9, Science (80-.). 346 (2014) 1258096, https://doi.org/10.1126/science.1258096.
[205] I. Kaushik, S. Ramachandran, S.K. Srivastava, CRISPR-Cas9: A multifaceted therapeutic strategy for cancer treatment, Semin. Cell Dev. Biol. 96 (2019) 4–12, https://doi.org/10.1016/j.semcdb.2019.04.018.
[206] M.F. Bolukbasi, A. Gupta, S.A. Wolfe, Creating and evaluating accurate CRISPR-Cas9 scalpels for genomic surgery, Nat. Methods 13 (2016) 41–50, https://doi.org/10.1038/nmeth.3684.
[207] M.M. Rahman, T.O. Tollefsbol, Targeting cancer epigenetics with CRISPR-dCAS9: Principles and prospects, Methods (2020), https://doi.org/10.1016/j.ymeth.2020.04.006.
[208] E. Yasun, Theranostic cancer applications utilized by nanoparticles offering multimodal systems and future insights, SN Appl. Sci. 2 (2020) 1–5.
[209] S. Aghamiri, S. Talaei, A.A. Ghavidel, F. Zandsalimi, S. Masoumi, N.H. Hafshejani, V. Jajarmi, Nanoparticles-mediated CRISPR/Cas9 delivery: Recent advances in cancer treatment, J. Drug Deliv. Sci. Technol. 56 (2020) 101533, https://doi.org/10.1016/j.jddst.2020.101533.
[210] T. Wan, D. Niu, C. Wu, F.-J. Xu, G. Church, Y. Ping, Material solutions for delivery of CRISPR/Cas-based genome editing tools: Current status and future outlook, Mater. Today (2019), https://doi.org/10.1016/j.mattod.2018.12.003.
[211] B. Liu, W. Ejaz, S. Gong, M. Kurbanov, M. Canakci, F. Anson, S. Thayumanavan, Engineered interactions with mesoporous silica facilitate intracellular delivery of proteins and gene editing, Nano Lett. 20 (2020) 4014–4021, https://doi.org/10.1021/acs.nanolett.0c01387.
[212] X. Xu, O. Koivisto, C. Liu, J. Zhou, M. Miihkinen, G. Jacquemet, D. Wang, J. M. Rosenholm, Y. Shu, H. Zhang, Effective delivery of the crispr/cas9 system enabled by functionalized mesoporous silica nanoparticles for gfp-tagged paxillin knock-in, Adv. Ther. 2000072 (2020), https://doi.org/10.1002/adtp.202000072.
[213] N.O. Deakin, C.E. Turner, Distinct roles for paxillin and Hic-5 in regulating breast cancer cell morphology, invasion, and metastasis, Mol. Biol. Cell 22 (2011) 327–341, https://doi.org/10.1091/mbc.E10-09-0790.
[214] Y. Ma, G. Mao, G. Wu, Z. Cui, X.-E. Zhang, W. Huang, CRISPR-dCas9-guided and telomerase-responsive nanosystem for precise anti-cancer drug delivery, ACS Appl. Mater. Interfaces 13 (2021) 7890–7896, https://doi.org/10.1021/acsami.0c19217.